The Plant Cell, Vol. 29: 1053–1072, May 2017, www.plantcell.org © 2017 ASPB.

Ethylene-Inhibited Jasmonic Acid Biosynthesis Promotes Mesocotyl/Coleoptile Elongation of Etiolated Rice Seedlings[OPEN]

Qing Xiong,[a,b,1] Biao Ma,[a,1,2] Xiang Lu,[a,b,1] Yi-Hua Huang,[a,b] Si-Jie He,[a] Chao Yang,[a] Cui-Cui Yin,[a] He Zhao,[a,b] Yang Zhou,[a,b] Wan-Ke Zhang,[a] Wen-Sheng Wang,[c] Zhi-Kang Li,[c] Shou-Yi Chen,[a,2] and Jin-Song Zhang[a,b,2]

[a] State Key Lab of Plant Genomics, Institute of Genetics and Developmental Biology, Chinese Academy of Sciences, Beijing 100101, China

[b] University of Chinese Academy of Sciences, Beijing 100049, China

[c] Institute of Crop Sciences/National Key Facilities for Crop Gene Resources and Genetic Improvement, Chinese Academy of Agricultural Sciences, Beijing 100081, China

ORCID IDs: 0000-0003-4222-4371 (H.Z.); 0000-0003-3475-2852 (W.-K.Z.); 0000-0003-2165-3468 (J.-S.Z.)

Elongation of the mesocotyl and coleoptile facilitates the emergence of rice (*Oryza sativa*) seedlings from soil and is affected by various genetic and environment factors. The regulatory mechanism underlying this process remains largely unclear. Here, we examined the regulation of mesocotyl and coleoptile growth by characterizing a *gaoyao1* (*gy1*) mutant that exhibits a longer mesocotyl and longer coleoptile than its original variety of rice. *GY1* was identified through map-based cloning and encodes a PLA_1-type phospholipase that localizes in chloroplasts. GY1 functions at the initial step of jasmonic acid (JA) biosynthesis to repress mesocotyl and coleoptile elongation in etiolated rice seedlings. Ethylene inhibits the expression of *GY1* and other genes in the JA biosynthesis pathway to reduce JA levels and enhance mesocotyl and coleoptile growth by promoting cell elongation. Genetically, *GY1* acts downstream of the OsEIN2-mediated ethylene signaling pathway to regulate mesocotyl/coleoptile growth. Through analysis of the resequencing data from 3000 rice accessions, we identified a single natural variation of the *GY1* gene, $GY1^{376T}$, which contributes to mesocotyl elongation in rice varieties. Our study reveals novel insights into the regulatory mechanism of mesocotyl/coleoptile elongation and should have practical applications in rice breeding programs.

INTRODUCTION

Flowering plants begin their life cycle as a seed beneath the soil surface. With adequate water and proper temperature, the seeds germinate and seedlings develop. The seedlings withstand complex environments to emerge from the soil and initiate their growth in light. For rice (*Oryza sativa*), the coleoptile is an essential structure of the seedlings that protects the plumule as it moves through the soil layers. Below the coleoptile, a short stem, also called the mesocotyl, develops in the dark, which pushes the base of the coleoptile toward the soil surface. The elongation of the mesocotyl and coleoptile is regulated by various genetic and environmental factors, which stimulate the emergence of rice seedlings (Takahashi, 1978; Helms et al., 1989; Dilday et al., 1990).

Plant hormones and other related factors affect the growth of the mesocotyl and coleoptile. For instance, abscisic acid promotes mesocotyl growth through increasing the cell division activity of the meristem (Watanabe et al., 2001). Strigolactones inhibit mesocotyl growth through inhibiting cell division, and cytokinin antagonizes strigolactones to regulate mesocotyl elongation (Hu et al., 2010, 2014). The photoreceptor mutant *osphyA-1* exhibits longer mesocotyls and coleoptiles under continuous far-red light (Takano et al., 2001). Furthermore, light inhibits mesocotyl and coleoptile growth by regulating jasmonic acid (JA) biosynthesis (Svyatyna and Riemann, 2012). Mutants of *OsAOS1/CPM1*, *OsAOC/CPM2*, and *OsJAR1/OsGH3.5*, which are involved in JA biosynthesis (Svyatyna and Riemann, 2012), showed a longer coleoptile phenotype under red light (Biswas et al., 2003; Riemann et al., 2003, 2008; Svyatyna and Riemann, 2012). Expansins are cell wall-loosening proteins that induce wall stress relaxation and volumetric extension of plant cells (Cho and Cosgrove, 2000; Li et al., 2003). Expansins are encoded by substantial gene families and have classically been divided into two subfamilies, α- and β-expansins (Li et al., 2003). Overexpression of *AtEXP4* in transgenic *Arabidopsis thaliana* plants led to slightly longer petioles, larger leaf blades, and larger cells than controls (Cho and Cosgrove, 2000). Overexpressing the expansin gene *OsEXP4* promoted elongation of the mesocotyl and coleoptile in rice (Choi et al., 2003).

Recent studies of seedling emergence in Arabidopsis suggest that ethylene regulates etiolated growth and the seedlings' response to soil through interacting with photomorphogenesis factors (Zhong et al., 2014; Shi et al., 2016a, 2016b). Ethylene is an important gaseous plant hormone that regulates various processes in plant growth and development (Bleecker and Kende, 2000; Guo and Ecker, 2004; Rzewuski and Sauter, 2008; Ma et al., 2010). In Arabidopsis, the perception of ethylene is based on the binding of ethylene to its five membrane receptors (Hua and Meyerowitz, 1998). After perception, a negative regulator,

[1] These authors contributed equally to this work.

[2] Address correspondence to jszhang@genetics.ac.cn, sychen@genetics.ac.cn, or mabiao@genetics.ac.cn.
The author responsible for distribution of materials integral to the findings presented in this article in accordance with the policy described in the Instructions for Authors (www.plantcell.org) is: Jin-Song Zhang (jszhang@genetics.ac.cn).

[OPEN] Articles can be viewed without a subscription.
www.plantcell.org/cgi/doi/10.1105/tpc.16.00981

CONSTITUTIVE TRIPLE RESPONSE1, is repressed (Kieber et al., 1993), and the central signal transducer ETHYLENE-INSENSITIVE2 (EIN2) is cleaved at the C-terminal end. This C-terminal end is further translocated into the nucleus for activation of transcription factors EIN3/EIN3-Like 1 (EIN3/EIL1) (Chao et al., 1997; Alonso et al., 1999; Ju et al., 2012; Qiao et al., 2012; Wen et al., 2012). EIN2 also enters the P-body, where it represses the translation of EIN3 Binding F-Box 1/2, which in turn stabilizes EIN3/EIL1 and thereby activates diverse ethylene responses (Li et al., 2015). Our previous studies demonstrated that *MaoHuZi7* (*MHZ7*/*OsEIN2*), *MHZ6*/*OsEIL1*, and *OsEIL2* regulate root and coleoptile growth in rice etiolated seedlings (Ma et al., 2013; Yang et al., 2015b).

Ethylene and JA regulate plant growth, development, and defense responses, both synergistically and antagonistically (Song et al., 2014a; Liu et al., 2015; Yang et al., 2015a). The induction of *PLANT DEFENSIN 1.2* and *ETHYLENE RESPONSE FACTOR1* relies on both ethylene and JA (Penninckx et al., 1998; Lorenzo et al., 2003). Ethylene and JA both promote root hair growth (Zhu et al., 2006). Furthermore, JA promotes the degradation of Jasmonate-ZIM domain protein (JAZ), which interacts with and represses EIN3/EIL1, suggesting a synergistic regulation between ethylene and JA (Zhu et al., 2011). Recently, EIN3 and MYC2 have been found to interact with each other at different levels to regulate the antagonism between ethylene and JA in Arabidopsis (Song et al., 2014a, 2014b; Zhang et al., 2014).

The biosynthesis of JA initiates with phospholipases in chloroplasts, which release α-linolenic acid from the chloroplast membrane (Wang et al., 2000; Hyun et al., 2008; Ellinger et al., 2010; Liu et al., 2015). The lipoxygenases (LOXs) then oxidate α-linolenic acid to produce 13-hydroperoxy-octadecatrienoic acid (13-HPOT) and 9-HPOT (Feussner and Wasternack, 2002; Bannenberg et al., 2009; Chauvin et al., 2013). After allene oxide synthase converts hydroperoxides to an unstable 12,13 (*S*)-epoxylinolenic acid, the allene oxide cyclase catalyzes the conversion of the product to (9*S*,13*S*)-12-oxo-phytodienoic acid (Ziegler et al., 2000), which is later transferred into peroxisomes and reduced to OPC-8:0 by 12-oxophytodienoic acid reductase (OPR) (Schaller et al., 2000). The OPC-8:0 is esterified with CoA by OPC-8:CoA ligase 1 (OPCL1) and then subjected to three cycles of β-oxidation, which involves the action of acyl-CoA oxidase, the multifunctional protein, and 3-ketoacyl-CoA thiolase to generate JA (Hayashi et al., 1999; Eastmond and Graham, 2000; Eastmond et al., 2000; Schaller and Stintzi, 2009). The active form of JA, jasmonoyl-isoleucine, is synthesized by JAR1 through activating the amide-linked conjugation of the carboxyl group to Ile (Staswick et al., 2002).

Although interactions between ethylene and JA affect various responses, their roles in mesocotyl/coleoptile elongation and the emergence of rice seedlings are not known. In this study, we identified and characterized the rice mutant *gaoyao1* (*gy1*), which exhibits long mesocotyls and long coleoptiles. Through map-based cloning, we found that *GY1* encodes a phospholipase that functions at the initial step of the JA biosynthesis pathway. JA inhibits mesocotyl/coleoptile elongation, and ethylene suppresses JA biosynthesis to promote mesocotyl/coleoptile growth. We further identified a single elite allele of *GY1* from 3000 rice accessions and found that this allele is associated with long mesocotyls of rice seedlings. Our study reveals a mechanism by which the mesocotyl and coleoptile elongate when rice seedlings emerge from the soil and should facilitate breeding for new rice cultivars that are adapted to growing in dry soil.

RESULTS

The *gy1* Mutant Has Longer Mesocotyls and Coleoptiles

In screening for ethylene response mutants in rice (*O. sativa* cv Nipponbare), a mutant exhibiting longer mesocotyl and longer coleoptile than the wild-type Nipponbare (Nip) in etiolated seedlings was identified and named *gaoyao1* (a Chinese name meaning high waist) (Figures 1A and 1B). In a backcross of the *gy1* mutant with Nip, all members of the F1 generation exhibited a wild-type phenotype, and the F2 generation segregated at a ratio of 3:1 (wild-type phenotype:mutant phenotype) (Supplemental Table 1), indicating that the mutant harbors a recessive mutation in a single gene. However, the *gy1* mutant seemed to exhibit normal ethylene response and had similar ethylene production in comparison to Nip (Supplemental Figures 1A to 1C).

Long mesocotyls and coleoptiles may facilitate the emergence of rice seedlings from the soil (Dilday et al., 1990). We then measured the emergence rate of the *gy1* mutant and Nip. The germinated seeds were sown in potted soil at a depth of 2 cm at 28°C. Three days later, about half of the *gy1* mutant seedlings had emerged from the soil, while only a few Nip seedlings had emerged (Figure 1C). At a later stage, all the Nip and *gy1* mutants emerged and the *gy1* mutant seedlings were significantly taller than Nip seedlings at all stages examined (Supplemental Figure 2). Three-day-old seedlings were removed from the soil and compared. The *gy1* mutant has much longer mesocotyls than Nip, and the difference in mesocotyl length was greater in soil-grown etiolated seedlings than that in water-grown etiolated seedlings (Figures 1A, 1B, 1D, and 1E). These results indicate that the longer mesocotyl and coleoptile in the *gy1* mutant may facilitate early emergence of seedlings from soil.

Map-Based Cloning of *GY1*

Although we used a rice T-DNA-tagged population for mutant screening, most of our identified mutants harbored point and/or short InDel mutations (Ma et al., 2013, 2014; Yang et al., 2015b; Yin et al., 2015), which are most likely generated during mass production of rice embryogenic calli and longer callus growth periods (Wei et al., 2016). The tagging efficiency of T-DNA-tagged populations is only 5 to 10% in rice, and the relationship between flanking sequence and phenotype is very weak (Wei et al., 2016). Based on our previous studies (Ma et al., 2013, 2014; Yang et al., 2015b; Yin et al., 2015), map-based cloning was used to identify the gene responsible for the *gy1* phenotype. Using 927 individuals with the *gy1* phenotype segregated in the F2 population derived from a cross between the *gy1* mutant and an *indica* cultivar TN1, the *GY1* locus was located to a 48-kb region of chromosome 1. This region contained three predicted genes, according to information in the rice genome annotation project (http://rice.plantbiology.msu.edu/). None of these genes was differentially expressed between Nip and the *gy1* mutant (Supplemental Figure 1D). Genome sequencing indicated that

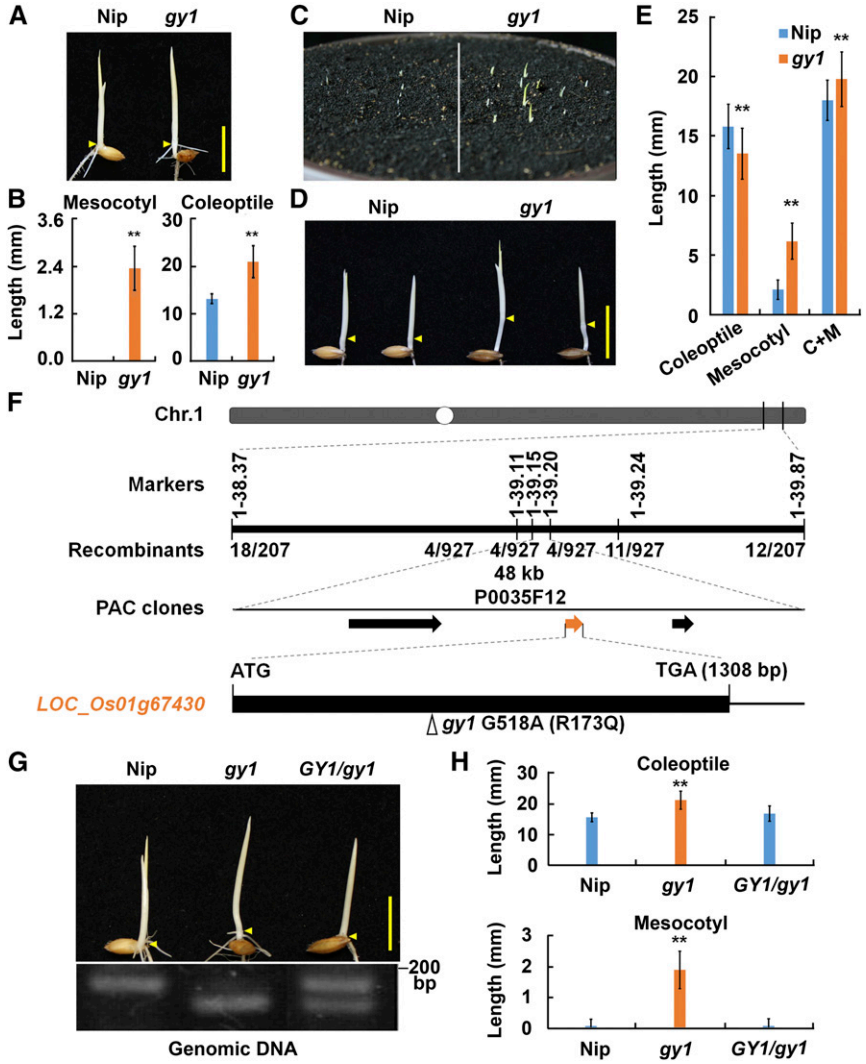

Figure 1. Phenotype of the *gy1* Mutant and Map-Based Cloning of *GY1*.

(A) Comparison of Nip and *gy1* etiolated seedlings grown in water for 3 d after germination in darkness. Arrowheads indicate positions of coleoptilar nodes between the mesocotyl and coleoptile. Bars = 10 mm.

(B) Mesocotyl and coleoptile length of etiolated seedlings represented in **(A)**. The values are means ± SD of 20 to 30 seedlings per sample. The asterisks indicate significant difference compared with Nip (**P < 0.01, Student's *t* test).

(C) Emergence of Nip and *gy1* from soil. Germinated seeds were sown at a depth of 2 cm and seedlings were grown for 3 d under a 14-h-light/10-h-dark photoperiod.

(D) Etiolated Nip and *gy1* seedlings grown in soil as in **(C)**. Arrowheads indicate positions of coleoptilar nodes between the mesocotyl and coleoptile. Bar = 10 mm.

(E) Coleoptile and mesocotyl length of etiolated seedlings represented in **(D)**. The values are means ± SD of 20 to 30 seedlings per sample. The asterisks indicate significant difference compared with Nip (**P < 0.01, Student's *t* test).

(F) Map-based cloning of *GY1*. The *GY1* locus was mapped to a 48-kb region between marker 1-39.15 and marker 1-39.20 of chromosome 1. The numbers below the markers indicate the number of recombinant individuals among the examined individuals with the mutant phenotype from the F2 segregated population. The mutation site of *gy1* (G518A for nucleotide change and R173Q for amino acid change) is indicated by an arrowhead in the schematic diagram of *GY1*. The black box represents the coding region of *GY1*.

(G) The *GY1* genomic sequence complemented the *gy1* mutant phenotype. Etiolated seedlings from Nip, *gy1*, and the *GY1*-complemented line of *gy1* grown for 3 d after germination are shown. Arrowheads indicate positions of nodes. The lower panel is the confirmation of the transgenic line by cleaving PCR products with *Aor*51H I. The PCR products were amplified with the dCAPS primers listed in Supplemental Table 7. Bar = 10 mm.

(H) Coleoptile and mesocotyl length of etiolated seedlings represented in **(G)**. The values are means ± SD of 20 to 30 seedlings per sample. The asterisks indicate significant difference compared with Nip (**P < 0.01, Student's *t* test).

the *gy1* mutant had a single base substitution at 518 bp in a predicted putative lipase gene *LOC_Os01g67430*. This single base substitution of G to A in *gy1* resulted in mutation of GY1 at 173th amino acid, from arginine (R) to glutamine (Q) (R173Q) (Figure 1F).

To test whether this putative lipase gene could rescue the phenotype of the *gy1* mutant, a plasmid (*pC-GY1*) harboring the genomic sequence of the candidate gene, including the coding region and the 2022-bp upstream and 1476-bp downstream regions, was transformed into the *gy1* mutant plants. Transgenic plants showed complete complementation of the *gy1* phenotype at the seedling and mature stages (Figures 1G and 1H; Supplemental Figure 3). These results indicate that *GY1* is located at the LOC_Os01g67430 locus and encodes a putative lipase.

Spatial Expression of *GY1* and Protein Subcellular Localization

The expression pattern of *GY1* was analyzed in organs of Nip plants from the vegetative to reproductive stages using qPCR. *GY1* was highly expressed in the true leaf and coleoptile of etiolated seedlings, and exhibited much lower expression levels in the other organs examined (Figure 2A). In soil-grown etiolated seedlings, *GY1* expression was also higher in coleoptiles than in the other tested organs (Figure 2A). This result suggests that GY1 plays important roles in coleoptiles.

GY1 protein was predicted to localize in the chloroplasts using LocTree3 (Supplemental Figure 4A). To examine the cellular localization of GY1, a rice protoplast transient assay was performed using the pBI-*GY1-GFP* construct in which the GY1 coding sequence was fused in frame with GFP to generate a GY1:GFP fusion protein. The fluorescence signals of the GY1:GFP fusion protein colocalized with the chlorophyll red autofluorescence in the chloroplasts of rice and Arabidopsis protoplasts (Figure 2B; Supplemental Figure 4B). These results suggest that GY1 localizes in the chloroplast. While the materials used for rice protoplast preparation were etiolated seedlings, and the protoplasts were only cultured in light for a few hours during plasmid transformation, we deduce that GY1 may localize in the etioplasts of etiolated seedlings.

The Lipid Substrates of Phospholipase A1 Accumulated in the *gy1* Mutant

GY1 has no intron and encodes a putative phospholipase composed of 425-amino acid residues according to information from the NCBI database (http://www.ncbi.nlm.nih.gov/) (Figure 2C). Homology searches with GY1 amino acid sequences revealed that GY1 was similar to two Arabidopsis lipases, DONGLE (DGL) and DEFECTIVE IN ANTHER DEHISCENCE1 (DAD1). Both of these lipases belong to the phospholipase A1 (PLA_1) family (Figure 2D) (Hyun et al., 2008), whose members are characterized by the presence of a highly conserved GXSXG motif and a catalytic triad composed of a serine (S), an aspartic acid (D), and a histidine (H) residue (Singh et al., 2012). The GY1 protein contained a GHSMG motif and a putative catalytic triad S, D, and H that fit the definition of a PLA_1, suggesting that GY1 belongs to the PLA_1 family. Through multiple alignment of GY1 and its homologs, we found that the mutation site in the *gy1* mutant at the 173th amino acid was a highly conserved residue in all of the compared proteins from rice and Arabidopsis (Figure 2D).

Because GY1 is a member of the PLA_1 family, its mutation should affect the lipid profile. Lipid analysis of the *gy1* mutant and Nip showed that the levels of different species of phosphatidylcholine (PC), digalactosyldiacylglycerol, and monogalactosyldiacylglycerol, the main substrates of PLA_1 (Singh et al., 2012), were significantly higher in the *gy1* mutant than in Nip (Figures 3A to 3D). These results imply that the point mutation in the *gy1* mutant affects the PLA_1 activity of the GY1.

GY1 Mediates the Initial Step of JA Biosynthesis

Since GY1 clusters with AtDGL (Supplemental Figure 5 and Supplemental Data Set 1), which is the first enzyme in the JA biosynthesis pathway, we predict that GY1 also initiates JA biosynthesis in rice. The JA contents in the etiolated seedlings of Nip and the *gy1* mutant were then measured to examine whether the *GY1* mutation hampered JA accumulation. The JA content was significantly lower in the shoots of *gy1* etiolated seedlings than in those of Nip etiolated seedlings, indicating that mutation in *GY1* blocked JA production (Figure 3E). *osaoc*, which harbors a mutation in the gene encoding a downstream JA biosynthesis enzyme OsAOC (Riemann et al., 2013), also exhibited longer mesocotyls and coleoptiles in etiolated seedlings than its wild-type Nihonmasari (Supplemental Figure 6). These results indicate that disruption of the JA biosynthesis pathway underlies the long mesocotyl and long coleoptile phenotype of etiolated seedlings.

To further examine the role of JA in mesocotyl/coleoptile growth regulation, we investigated whether JA application could rescue the *gy1* mutant phenotype. A concentration of 1 μM MeJA was selected because this level did not affect coleoptile growth of Nip seedlings (Supplemental Figure 7). With 1 μM MeJA treatment, the *gy1* mutant phenotype was almost completely recovered and resembled Nip seedlings (Figure 3F), and the lengths of *gy1* mesocotyls and coleoptiles were similar to those of Nip mesocotyls and coleoptiles of seedlings of the same age under normal growth conditions (Figure 3G). These results indicate that GY1 is a PLA_1 family protein mediating the initial step of the JA biosynthesis pathway, and JA represses mesocotyl and coleoptile elongation in etiolated rice seedlings.

Emergence of Rice Seedlings Correlates with Reduced Jasmonic Acid Content but Increased Ethylene Production

Considering that the longer mesocotyl and coleoptile of the *gy1* mutant facilitate seedling emergence from soil (Figures 1C and 1D; Supplemental Figure 2), disruption of JA biosynthesis leads to mesocotyl and coleoptile elongation (Figures 1A and 1B and Figure 3E; Supplemental Figure 6), JA application rescued the *gy1* mutant phenotype (Figures 3F and 3G), and soil-grown Nip seedlings have longer mesocotyls than the water-grown Nip seedlings (Figures 1A, 1B, 1D, and 1E), we speculated that JA content may be related to the emergence process of rice seedlings from under the soil.

The germinated Nip seeds were sown in pots covered with different depths of soil (0, 1, and 2 cm) and grown for 3 d, and

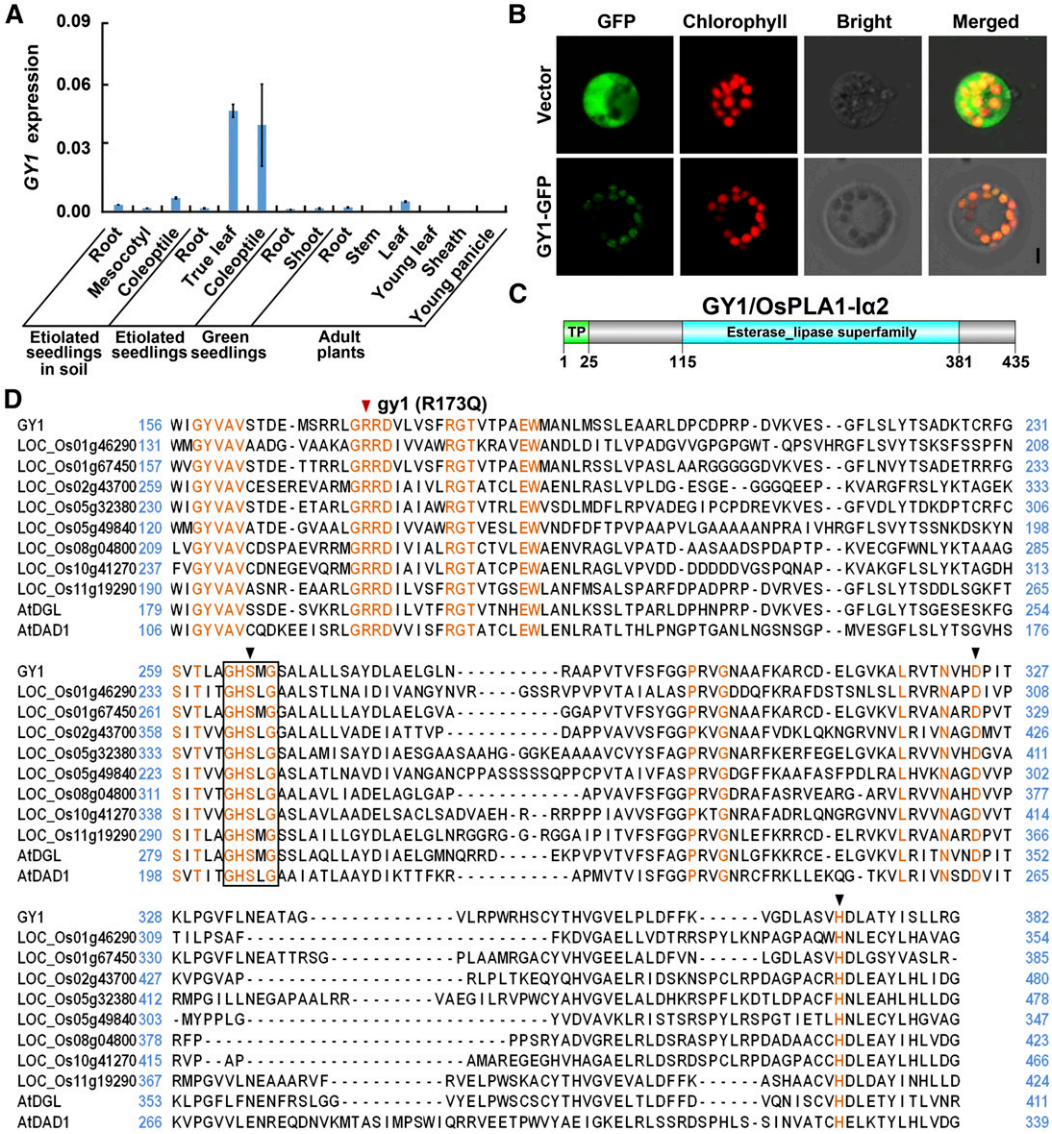

Figure 2. *GY1* Expression, Protein Subcellular Localization, and Alignment Analysis of GY1 with Its Homologs.

(A) *GY1* expression level in different organs of Nip detected by qPCR relative to *OsActin2* expression. "Etiolated seedlings in soil" indicate that the germinated seeds were sown in soil at a depth of 4 cm. "Etiolated seedlings" and "Green seedlings" represent seedlings cultured under regular water conditions in darkness and in 14 h light/10 h dark, respectively. "Adult plants" represent plants grown in the field. The values are means ± SD of three biological replicates (independent pools of tissue) per sample.

(B) GY1 is localized in chloroplasts of rice protoplasts as revealed by the merged green fluorescence of GY1-GFP fusion protein and the red auto-fluorescence of chlorophyll. Bar = 5 μm.

(C) A schematic diagram of GY1 protein. A transit peptide (TP) and an esterase/lipase domain are indicated.

(D) Alignment of GY1 and its homologs. Multiple alignments of amino acid sequences of GY1 and its homologs in rice and Arabidopsis were conducted using MEGA6. Identical residues are shaded in orange. The black box indicates the highly conserved GXSXG motif of PLA_1. The black arrowheads indicate a triad of amino acids in the catalytic center of PLA_1. The red arrowhead indicates the mutation site (R173Q) in *gy1*.

then the seedlings were removed for evaluation. The length of the mesocotyl and coleoptile increased with increasing seed-sowing depth (Figures 4A and 4B). The JA content and *GY1* expression level were also measured in this process, and values from both parameters decreased drastically at greater soil depths (Figures 4C and 4D). These results suggest that less JA promotes the emergence of rice seedlings from thicker soil cover.

We previously revealed that *MHZ7*/*OsEIN2*-overexpressing rice seedlings exhibited the long mesocotyl and long coleoptile phenotype upon ethylene treatment (Ma et al., 2013), resembling the *gy1* mutant (Figure 1A). In Arabidopsis

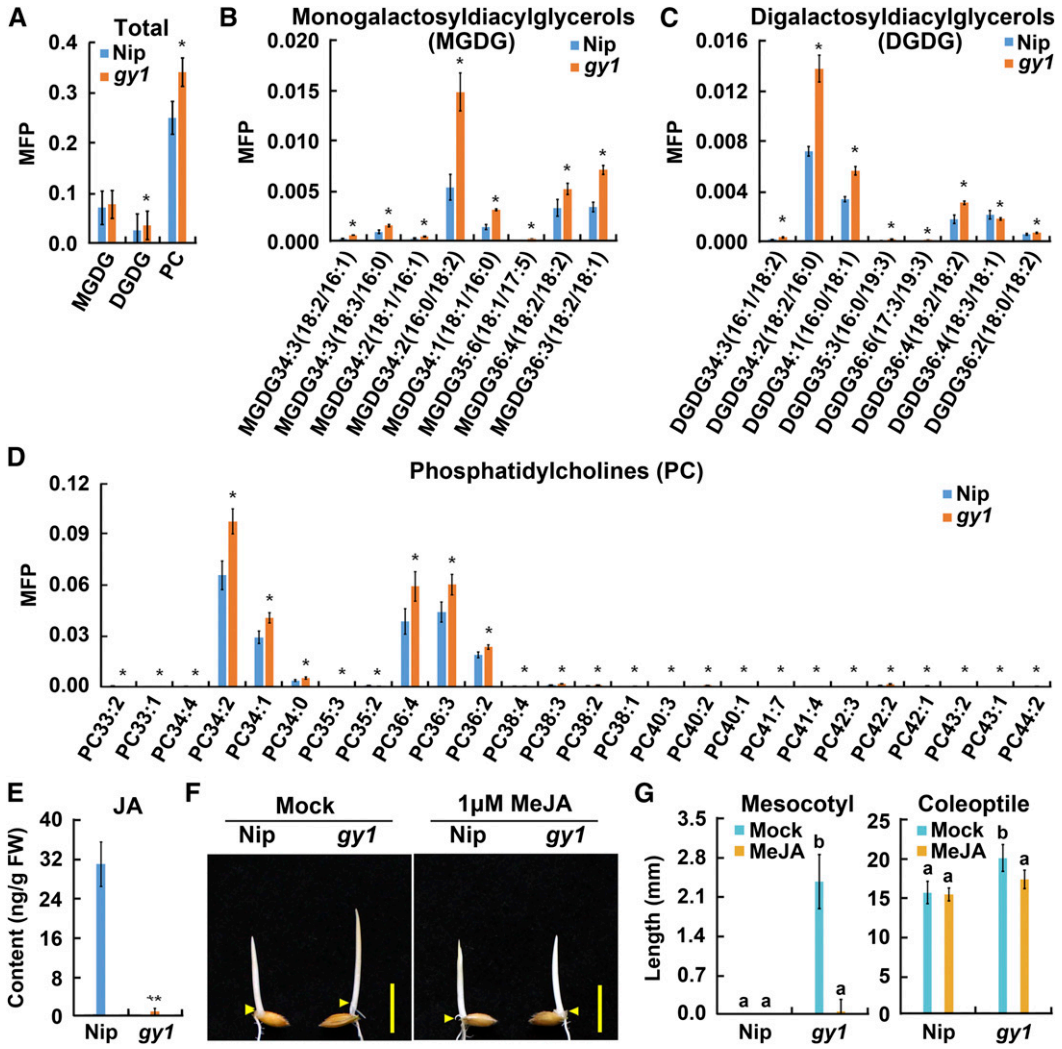

Figure 3. Lipid Contents and JA Contents in Rice Seedlings and MeJA Rescue of *gy1* Phenotype.

(A) Total monogalactosyldiacylglycerols (MGDG), digalactosyldiacylglycerols (DGDG), and PC levels expressed in molar fractions normalized to total polar lipids (MFP) in etiolated seedlings from Nip and gy1 grown for 3 d after germination in dark. The values are means ± SD of four biological replicates (independent pools of tissue) per sample. The asterisks indicate significant difference compared with the corresponding values in Nip (*P < 0.05, Student's *t* test).

(B) Levels of monogalactosyldiacylglycerol species in etiolated seedlings of Nip and *gy1*. Other indications are as in **(A)**.

(C) Levels of digalactosyldiacylglycerol species in etiolated seedlings of Nip and *gy1*. Other indications are as in **(A)**.

(D) Levels of PC species in etiolated seedlings from Nip and *gy1*. Other indications are as in **(A)**.

(E) JA content in etiolated seedlings from Nip and *gy1* grown for 3 d after germination in dark. The values are means ± SD of three biological replicates (independent pools of tissue) per sample. The asterisks indicate significant difference compared with Nip (**P < 0.01, Student's *t* test).

(F) MeJA (1 μM) treatment rescued *gy1* phenotype. The etiolated seedlings were grown for 3 d after germination in dark. Arrowheads indicate positions of the coleoptilar nodes between mesocotyl and coleoptile. Bar = 10 mm.

(G) Mesocotyl and coleoptile length of etiolated seedlings represented in **(F)**. The values are means ± SD of 20 to 30 seedlings per sample. Different letters above each column indicate significant difference between the compared pairs (P < 0.05, Student's *t* test).

seedlings, ethylene production was activated by soil cover (Zhong et al., 2014). Based on these findings, we propose that the GY1-mediated JA biosynthesis that inhibits mesocotyl and coleoptile elongation may be related to the ethylene pathway. We then examined ethylene production during rice seedling emergence when seedlings were sown at the same soil depths, from 0 to 2 cm. Ethylene emission increased in the rice seedlings with increasing seed-sowing depth (Figure 4E).

All these results indicate that, when rice seedlings are covered with soil, ethylene production is induced, whereas JA biosynthesis is inhibited, and that these changes in hormone production promote the elongation of mesocotyls and coleoptiles of rice seedlings, facilitating their emergence from soil.

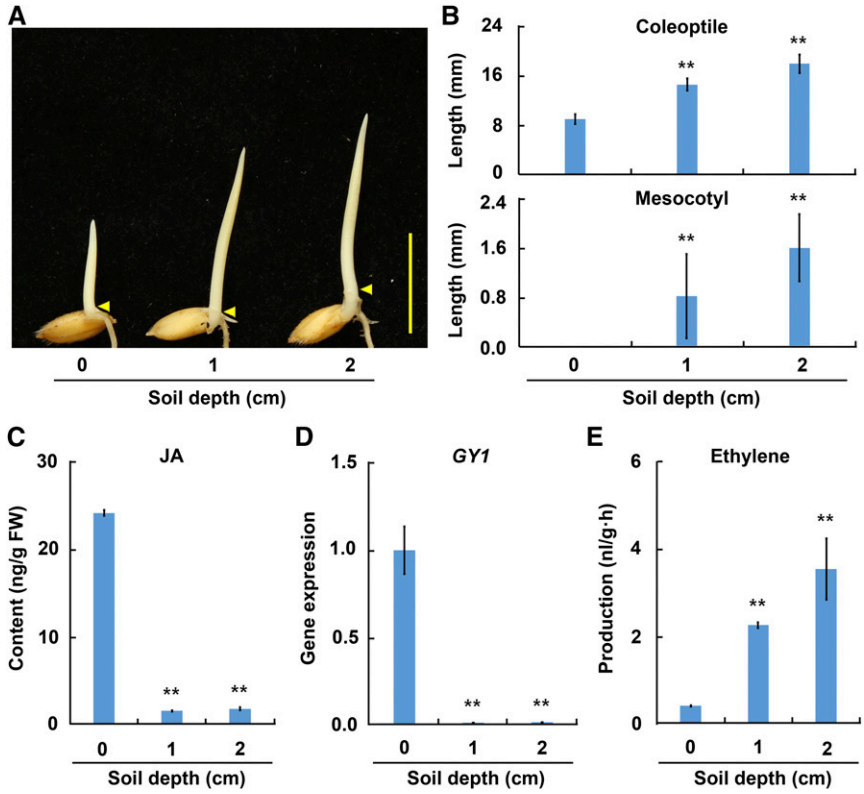

Figure 4. Phenotypic and Hormone Changes in Rice Seedlings after Seed-Sowing at Different Soil Depths.

(A) Comparison of Nip etiolated seedlings sown at different depths in soil. The germinated seeds were covered with 0, 1, and 2 cm soil and the seedlings were grown for 3 d in darkness. Arrowheads indicate positions of coleoptilar nodes between the mesocotyl and coleoptile. Bar = 10 mm.

(B) Coleoptile and mesocotyl length of Nip etiolated seedlings represented in **(A)**. The values are means ± SD of 20 to 30 seedlings per sample. The asterisks indicate significant difference compared with the "0 cm" value (**P < 0.01, Student's *t* test).

(C) JA contents in shoots of Nip seedlings sown at different depths. The values are means ± SD of three biological replicates (independent pools of tissue) per sample. The asterisks indicate significant difference compared with the "0 cm" value (**P < 0.01, Student's *t* test).

(D) *GY1* relative expression in shoots of Nip seedlings sown at different depths. The expression was detected by qPCR relative to *OsActin2*. The values are means ± SD of three biological replicates (independent pools of tissue) per sample. The asterisks indicate significant difference compared with the "0 cm" value (**P < 0.01, Student's *t* test).

(E) Ethylene production in Nip seedlings sown at different depths. The values are means ± SD of three biological replicates (independent pools of tissue) per sample. The asterisks indicate significant difference compared with the "0 cm" value (**P < 0.01, Student's *t* test).

JA Biosynthesis Is Repressed by the Ethylene Pathway

To further explore the relationship between JA and ethylene during elongation of etiolated rice seedlings, we measured the JA content in the presence or absence of ethylene treatment. Under 10 ppm ethylene, the JA content in Nip etiolated seedlings decreased in comparison with that of the non-treatment control, whereas the JA content in *gy1* etiolated seedlings did not differ in the presence or absence of ethylene treatment (Figure 5A). *GY1* expression in 2-d-old etiolated seedlings was also significantly inhibited by ethylene after 3 to 12 h of treatment (Figure 5B). We further examined the expression of other genes in the JA biosynthesis pathway and all the tested genes were significantly inhibited by ethylene at different levels (Figure 5C). We also subjected deetiolated seedlings (etiolated seedlings exposed to light for 1 h) to the ethylene treatment. In these deetiolated seedlings, the JA content and expression of *GY1* and most other JA biosynthesis genes were higher than those in etiolated seedlings (Supplemental Figures 8A and 8B). After ethylene treatment, clear reductions in JA content and the expression of *GY1* and other JA biosynthesis genes were still observed in the deetiolated seedlings (Supplemental Figures 8A and 8B). All these results indicate that ethylene inhibits JA accumulation through suppressing the expression of *GY1* and other genes in the JA biosynthesis pathway.

To determine whether the inhibition of *GY1* by ethylene depends on the ethylene signaling pathway, we examined *GY1* expression in ethylene response mutants/RNAi plants and in plants overexpressing *MHZ7*/*OsEIN2* and *OsEIL2*, which were established in our previous studies (Ma et al., 2013; Yang et al., 2015b). MHZ7/OsEIN2 is homologous to EIN2, a central membrane protein in Arabidopsis ethylene signaling (Ma et al., 2013). OsEIL2 is homologous to the transcription factor EIN3 of the Arabidopsis ethylene signaling pathway and specifically regulates the coleoptile ethylene response of etiolated rice seedlings (Yang et al.,

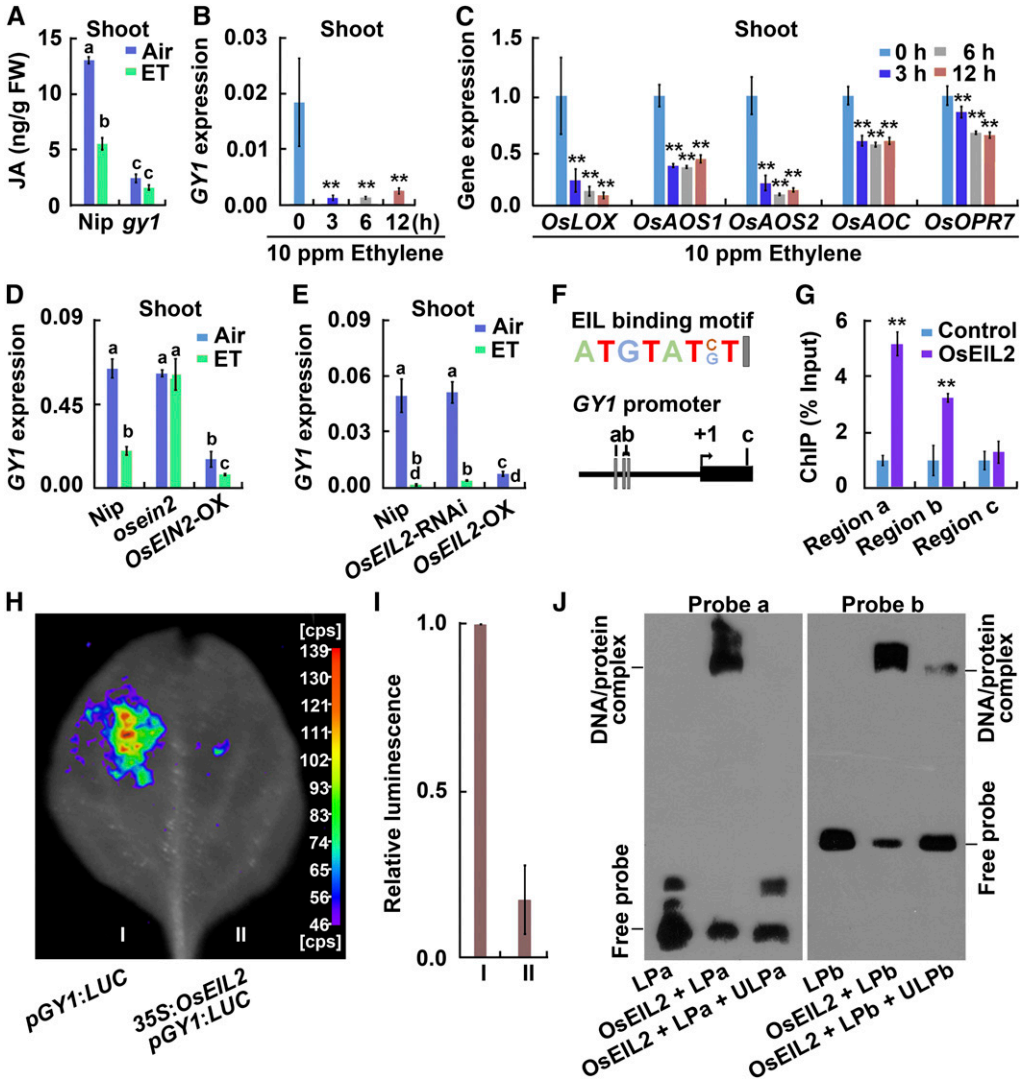

Figure 5. Ethylene Inhibits *GY1* Expression through OsEIL2.

(A) JA content in etiolated seedlings from Nip and *gy1* grown for 3 d after germination in darkness. ET indicates 10 ppm ethylene treatment for 8 h. The values are means ± SD of three biological replicates (independent pools of tissue) per sample. Different letters above each column indicate significant difference between the compared pairs ($P < 0.05$, Student's *t* test).

(B) *GY1* expression in shoots of Nip etiolated seedlings after 10 ppm ethylene treatment for 8 h. The quantitation was performed by qPCR relative to *OsActin2* expression. The values are means ± SD of three biological replicates (independent pools of tissue) per sample. The asterisks indicate significant difference compared with the "0 h" value (**$P < 0.01$, Student's *t* test).

(C) Expression of *OsLOX*, *OsAOS1*, *OsAOS2*, *OsAOC*, and *OsOPR7* from the JA biosynthesis pathway in shoots of etiolated Nip seedlings. The seedlings were treated with 10 ppm ethylene for 8 h, and the quantitation was performed by qPCR relative to *OsActin2* expression. The expression level of each gene at the "0 h" treatment was set to 1 and other values were compared with it. The values are means ± SD of three biological replicates (independent pools of tissue) per sample. The asterisks indicate significant difference compared with the "0 h" value (**$P < 0.01$, Student's *t* test).

(D) *GY1* expression level in the shoots of Nip, *mhz7*/*osein2*, and *MHZ7*/*OsEIN2*-OX etiolated seedlings after treatment with 10 ppm ethylene (ET) for 8 h. The quantitation was performed by qPCR relative to OsActin2 expression. The values are means ± SD of three biological replicates (independent pools of tissue) per sample. Different letters above each column indicate significant difference between the compared pairs ($P < 0.05$, Student's *t* test).

(E) *GY1* expression in etiolated seedlings from Nip, *OsEIL2*-RNAi, and *OsEIL2*-OX after 10 ppm ethylene treatment for 8 h. Other indications are as in **(D)**.

(F) The EIL binding motif in the *GY1* promoter region. a, b, and c indicate regions examined by ChIP-PCR in **(G)**. a and b also indicate probe a and probe b used in **(J)**, respectively.

(G) Enrichment fold of the ChIP-PCR signals from the regions shown in **(F)**. The ChIP analysis was performed with the wild-type Nip (Control) and *35S*:*OsEIL2*:*GFP* (OsEIL2) transgenic plants. Error bars indicate ± SD from three biological repeats (independent pools of tissue). Asterisks indicate that the difference between OsEIL2 value and control value is significant ($P < 0.01$, Student's *t* test).

2015b). The ethylene-mediated inhibition of *GY1* expression was blocked in the *mhz7*/*osein2* mutant, but not in the *OsEIL2*-RNAi etiolated seedlings (Figures 5D and 5E). Plants overexpressing *MHZ7*/*OsEIN2* and *OsEIL2* had low expression levels of *GY1* compared with Nip under normal conditions, and the gene expression was further reduced with ethylene treatment (Figures 5D and 5E). These results indicate that ethylene signaling represses *GY1* expression in a MHZ7/OsEIN2-dependent manner.

As OsEIL2 overexpression repressed *GY1* expression, we analyzed whether this transcription factor can bind to the *GY1* promoter and inhibit the promoter activity. In the promoter region of *GY1*, three EIL consensus sequences were identified (Figure 5F) (Zhong et al., 2009; Boutrot et al., 2010; Yang et al., 2015b). To assess whether OsEIL2 could bind to the EIL binding motif in the promoter of *GY1* in vivo, we performed chromatin immunoprecipitation (ChIP) analysis with the *35S*:*OsEIL2-GFP* transgenic rice plants. The ChIP-PCR signals were enriched at the OsEIL2 binding region containing the EIL binding motif in the *35S*:*OsEIL2-GFP* transgenic plants (Figure 5G). The 2022-bp fragment upstream of the ATG start codon of *GY1* was further cloned into the reporter plasmid that carried a *LUCIFERASE* (*LUC*) gene. The effector plasmid *35S*:*OsEIL2*, together with the *pGY1*:*LUC* reporter plasmid, were coinjected into tobacco (*Nicotiana tabacum*) leaves for a transient expression assay. OsEIL2 significantly decreased the LUC activity driven by the *GY1* promoter compared with the control (Figures 5H and 5I). These results suggest that OsEIL2 inhibits the *GY1* promoter activity. An electrophoresis mobility shift assay (EMSA) was further performed to test whether OsEIL2 could directly bind to the *GY1* promoter, and OsEIL2 was found to specifically bind to the two probes containing the EIL binding motif (Figure 5J). Taken together, these results suggest that OsEIL2 inhibits *GY1* expression through direct binding to the *GY1* promoter and suppression of *GY1* promoter activity.

Genetic Relationship between *GY1* and the Ethylene Signaling Gene *MHZ7*/*OsEIN2* in Rice

To further examine the genetic relationship between *GY1* and the ethylene signaling pathway, we generated the double mutant *gy1 osein2* through a genetic cross of *gy1* with *mhz7*/*osein2*, which was identified in our previous study (Ma et al., 2013). The etiolated seedlings of the double mutant *gy1 osein2* exhibited a long mesocotyl and long coleoptile, very similar to the *gy1* phenotype (Figures 6A and 6B). This result suggests that *GY1* acts downstream of *MHZ7*/*OsEIN2* to regulate the elongation of the mesocotyl and coleoptile in etiolated rice seedlings.

We further applied JA to the *MHZ7*/*OsEIN2*-overexpressing plants to test whether JA has any effects on *MHZ7*/*OsEIN2* function. With 1 μM MeJA treatment, the long mesocotyl and long coleoptile of *MHZ7*/*OsEIN2*-OX seedlings were largely suppressed (Figures 6C and 6D), indicating that ethylene signaling-promoted mesocotyl and coleoptile growth at least partially requires a reduction in JA levels. These results support the notion that the JA pathway acts downstream of the ethylene pathway to regulate mesocotyl and coleoptile growth in etiolated rice seedlings.

Altered Gene Expression and Cell Elongation Correlate with the Long Mesocotyl and Coleoptile of *gy1*

To understand the molecular aspects of mesocotyl/coleoptile elongation, the mesocotyls of 3-d-old etiolated Nip and *gy1* mutant seedlings, which had been sown under 4 cm of soil, were harvested for mRNA library preparation, sequencing, and further bioinformatics analysis. The differentially expressed genes between Nip and the *gy1* mutant were then analyzed. Through enrichment analysis for Gene Ontology terms, differentially expressed genes were significantly enriched in these categories: external encapsulating structure, extracellular region, cell wall, cell cycle, DNA metabolic process, response to endogenous stimulus, and response to stimulus (Supplemental Figure 9A). Expression of the JA biosynthesis-related gene *OsJMT* and JA-induced genes *OsJIP-1*, *OsJIP-2*, *OsJIP-3*, and *OsJIP-4* in the term "response to endogenous stimulus" was significantly lower in the *gy1* mutant than in Nip (Supplemental Figure 9B). By contrast, the expression of the expansin family of genes *OsEXPA2*, *OsEXPA4*, *OsEXPB4*, *OsEXPB6*, *OsEXPB11*, and *OsEXPLA1* in the term "cell wall" was significantly higher in the *gy1* mutant than in Nip (Supplemental Figure 9C). We further analyzed the expression of expansin family genes in the shoots of etiolated Nip, Nip subjected to 10 ppm ethylene treatment, *MHZ7*/*OsEIN2*-OX (Ma et al., 2013), and *gy1* mutant seedlings by qPCR. The latter three materials had long mesocotyls/coleoptiles. The expression of *OsEXPA2*, *OsEXPA4*, *OsEXPB4*, *OsEXPB6*, *OsEXPB11*, and *OsEXPLA1* was significantly increased in Nip subjected to ethylene treatment, *MHZ7*/*OsEIN2*-OX, and the *gy1* mutant compared with Nip (Figure 7A). These results suggest that a reduction in the expression of JA-responsive genes and upregulation of expansin genes are related to the elongation of the mesocotyl/coleoptile in etiolated rice seedlings.

Since the expansin family of genes mainly promote cell length (Huang et al., 2000; Choi et al., 2003; Li et al., 2003; Sharova, 2007),

Figure 5. (continued).

(H) OsEIL2 represses the promoter activity of *GY1* in a transient expression assay in tobacco leaves. 35S:OsEIL2 was used as an effector plasmid and pGY1:LUC as a reporter plasmid harboring the *GY1* promoter-driven *LUC*. More than five biological replicates (independent pools of tissue) were performed with similar results.

(I) Quantitative analysis of luminescence intensity in samples from **(G)**. The values are means ± SD of four biological replicates (independent pools of tissue). The asterisks indicate significant difference compared with the control (**P < 0.01, Student's *t* test).

(J) OsEIL2 protein binds to the promoter region of *GY1* containing the EIL binding site. GST-tagged OsEIL2 N terminus fusion protein (OsEIL2) was incubated with biotin-labeled DNA fragments (probe a and probe b), respectively. An excess of unlabeled probe (competitor) was also added to compete with the biotin-labeled promoter region for OsEIL2 binding. LPa indicates labeled probe a. ULPa indicates unlabeled probe a. LPb indicates labeled probe b. ULPb indicates unlabeled probe b. The upper bands are labeled probes bound with OsEIL2 protein.

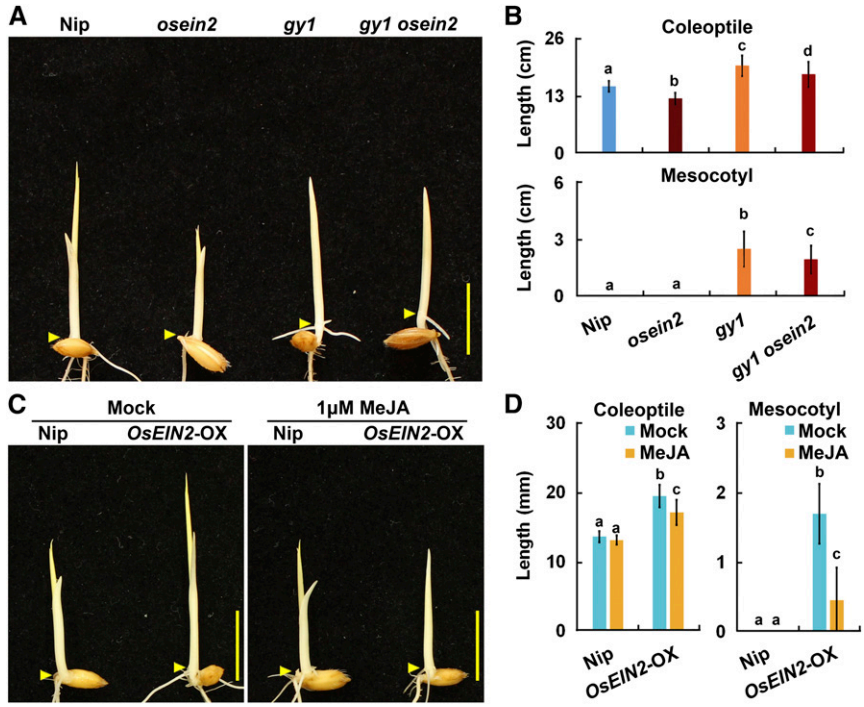

Figure 6. Genetic Interaction of *GY1* with *OsEIN2*.

(A) Etiolated Nip, *gy1*, *osein2*, and the *gy1 osein2* double mutant seedlings grown for 3 d after germination in darkness. Arrowheads indicate the coleoptilar nodes between the mesocotyl and coleoptile. Bar = 10 mm.

(B) Coleoptile and mesocotyl length of etiolated Nip, *gy1*, *osein2*, and *gy1 osein2* double mutant seedlings grown for 3 d after germination in darkness. The values are means ± SD of 20 to 30 seedlings per sample. Different letters above each column indicate significant difference between the compared pairs ($P < 0.05$, Student's *t* test).

(C) Etiolated seedlings from Nip and *MHZ7/OsEIN2*-OX without (mock) or with 1 μM MeJA treatment grown for 3 d after germination in darkness. Arrowheads indicate the coleoptilar nodes between the mesocotyl and coleoptile. Bar = 10 mm.

(D) Coleoptile and mesocotyl length of etiolated seedlings from Nip and *MHZ7/OsEIN2*-OX without (mock) or with 1 μM MeJA treatment grown for 3 d after germination in darkness. The values are means ± SD of 20 to 30 seedlings per sample. Different letters above each column indicate significant difference between the compared pairs ($P < 0.05$, Student's *t* test).

we examined the cell length of the etiolated seedlings from the above plants. The coleoptile cells of *MHZ7/OsEIN2*-OX and the *gy1* mutant were significantly longer than those of Nip under normal conditions, and ethylene treatment also increased the cell length of Nip (Figures 7B and 7C). These results indicate that the ethylene signaling pathway, as well as the *GY1* mutation, facilitates cell elongation to promote mesocotyl and coleoptile growth in rice seedlings.

A Natural Allelic Variation of *GY1* Contributes to Mesocotyl Elongation

Although *GY1* mutation-mediated mesocotyl elongation promotes emergence of seedlings, other yield-related agronomic traits were affected in the *gy1* mutant under field growth condition (Supplemental Table 2). We therefore investigated whether any natural variations of *GY1* are present, which are relevant to the long mesocotyl phenotype in etiolated seedlings of rice accessions. We meta-analyzed the coding sequence of *GY1* using the public resequencing data of 3000 rice accessions with representative diversity (Li et al., 2014). Compared with the Nip reference *GY1* sequence, we found that a single G376T single nucleotide polymorphism (SNP) existed in 141 rice accessions, which belonged to different rice subgroups and originated from different countries/regions in Asia, Africa, and South America (Figure 8A; Supplemental Table 3). This G376T SNP caused the 126th amino acid to change from glycine to cysteine. To assess whether the variation could influence the enzymatic activity, we measured the PLA activity of GY1, gy1 ($GY1^{518A}$), and $GY1^{376T}$. These results indicated that the PLA activity of gy1 and $GY1^{376T}$ was drastically lower than that of GY1. However, the PLA activity of $GY1^{376T}$ was significantly higher than that of gy1 (Figure 8B).

To elucidate whether the natural variant of 376T SNP in the *GY1* gene is associated with any change in mesocotyl phenotype in etiolated seedlings, we collected 51 available rice accessions from the above 141 rice accessions harboring the 376T SNP according to the public resequencing data and conducted an association analysis. These accessions belonged to different rice subgroups. We found that 44 rice accessions with 376T SNP exhibited a longer mesocotyl phenotype compared with Nip with 376G in *GY1*, whereas the other seven rice accessions exhibited a short mesocotyl phenotype like Nip. After resequencing the *GY1* gene

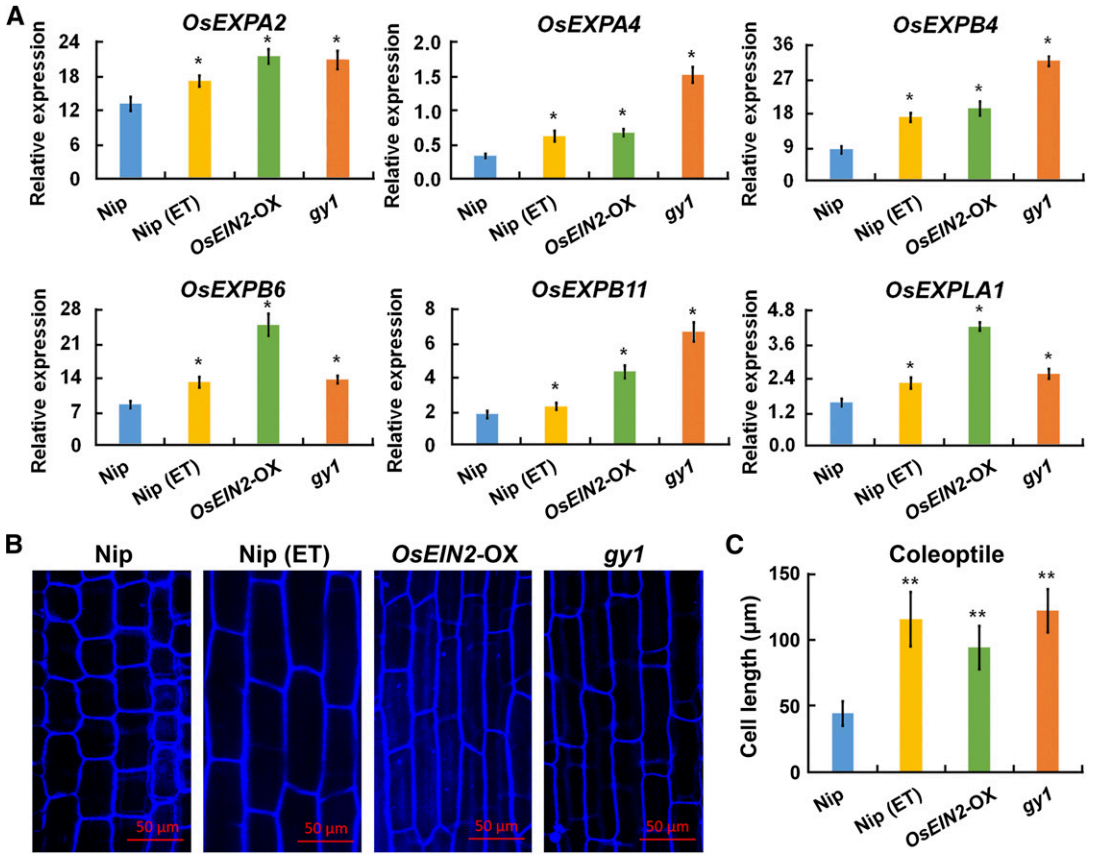

Figure 7. Expression of Expansin Family Genes and Cell Length of Coleoptiles in Different Seedlings.

(A) The expression level of *OsEXPA2*, *OsEXPA4*, *OsEXPB4*, *OsEXPB6*, *OsEXPB11*, and *OsEXPLA1* (*expansin-like A1*) in the shoots of etiolated Nip, Nip with 10 ppm ethylene (ET) treatment, *MHZ7/OsEIN2*-OX, and *gy1* seedlings, detected by qPCR relative to *OsActin2* expression. The values are means ± SD of three biological replicates (independent pools of tissue) per sample. The asterisks indicate significant difference compared with Nip ($P < 0.05$, Student's *t* test).

(B) Coleoptile cells of etiolated Nip, Nip with 10 ppm ethylene treatment, *MHZ7/OsEIN2*-OX, and *gy1* seedlings. Bar = 50 μm.

(C) Cell lengths of the coleoptiles of etiolated Nip, Nip with 10 ppm ethylene treatment, *MHZ7/OsEIN2*-OX, and *gy1* seedlings. The values are means ± SD of 20 to 30 cells per sample. The asterisks indicate significant difference compared with Nip (**$P < 0.01$, Student's *t* test).

in all 51 rice accessions, we found that the seven rice accessions exhibiting the short mesocotyl phenotype actually had the 376G SNP in their *GY1* gene (Figure 8C; Supplemental Figure 10 and Supplemental Table 4). These results indicate that the 376T SNP of the *GY1* gene correlates with the relatively long mesocotyls of etiolated rice seedlings.

Previously, five quantitative trait loci (QTL) for mesocotyl elongation were detected from backcross inbred lines developed from Kasalath and Nipponbare (Lee et al., 2012). The present *GY1* locus overlapped with one of them. Kasalath (with $GY1^{376T}$) etiolated seedlings also had a long mesocotyl and coleoptile, which were even longer than those of *gy1* probably due to increased cell elongation (Figures 8D to 8G; Supplemental Table 4).

To further demonstrate the role of GY1 in mesocotyl regulation, the *pC-GY1* plasmid used to complement the *gy1* mutant was transformed into Kasalath plants with the $GY1^{376T}$ genotype. The generated *GY1*-transgenic plants in the Kasalath background exhibited shorter mesocotyls and coleoptiles than Kasalath (Figures 8H and 8I). These transgenic plants also had higher levels of JA contents than Kasalath (Figure 8J). All the results suggest that the natural variant allele $GY1^{376T}$ of the *GY1* gene in Kasalath and other rice varieties is responsible for the long mesocotyl phenotype in etiolated seedlings.

DISCUSSION

In this study, we characterized the rice mutant *gy1* and revealed that JA inhibits the elongation of mesocotyls and coleoptiles of rice seedlings. During the emergence of rice seedlings from soil cover, ethylene production increases and GY1-mediated JA biosynthesis is then inhibited through the direct binding of OsEIL2 to the promoter region of *GY1*, ultimately promoting mesocotyl and coleoptile elongation of the rice seedlings. We found that an elite natural allele of *GY1* with the 376T SNP is associated with long mesocotyls and this finding may be used in breeding programs to select cultivars that can grow in dry land.

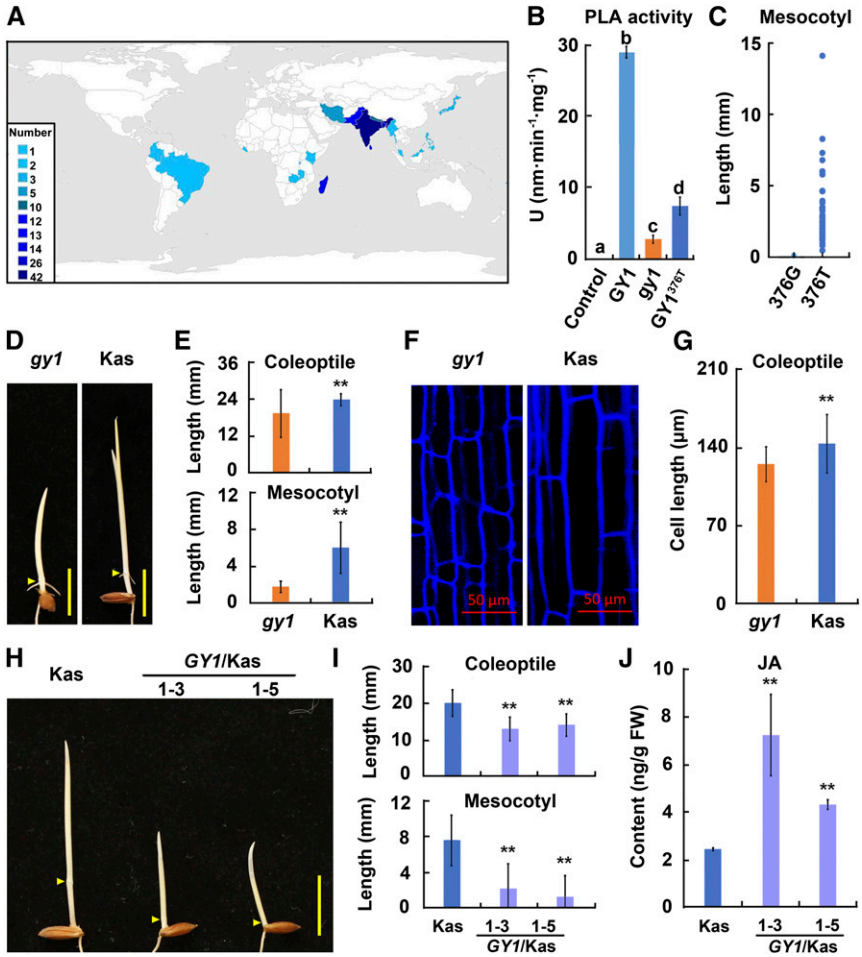

Figure 8. Natural Variation of *GY1* Correlates with Mesocotyl Elongation in Rice Accessions and GY1 Suppresses the Long Mesocotyl and Coleoptile Phenotypes in Kasalath Etiolated Seedlings.

(A) Distribution of the rice accessions harboring the 376T SNP in *GY1*. Countries are labeled with different shades of blue according to the number of varieties distributed in each country. The countries include Asian countries (India, Bangladesh, Sri Lanka, Pakistan, Nepal, Iran, Japan, Malaysia, Myanmar, and Philippines), African countries (Madagascar, Burundi, Kenya, Liberia, and Zambia), South American countries (Brazil and Colombia), and an Oceania country (Fiji).

(B) PLA activity of GY1, gy1 ($GY1^{518A}$), and $GY1^{376T}$. PLA activity was measured in vitro with dye-labeled PC as a substrate at 30°C. GY1, gy1 ($GY1^{518A}$), and $GY1^{376T}$ were expressed as fusion proteins with the SUMO peptide. SUMO peptide was used as a control. Values are means ± SD for four independent replicates. Different letters above each column indicate significant difference between the compared pairs ($P < 0.05$, LSD and S-N-K test).

(C) The 376T SNP of *GY1* correlates with long mesocotyls in rice accessions. The 376G SNP of *GY1* is related to short/no mesocotyl.

(D) Etiolated seedlings of *gy1* and Kasalath (Kas) grown for 3 d after germination in darkness. Arrowheads indicate the coleoptilar nodes between mesocotyl and coleoptile. Bar = 10 mm.

(E) Coleoptile and mesocotyl length of etiolated seedlings from **(C)**. The values are means ± SD of 20 to 30 seedlings per sample. The asterisks indicate significant difference compared with *gy1* (**$P < 0.01$, Student's *t* test).

(F) Coleoptile cells of etiolated seedlings from *gy1* and Kas. Bar = 50 μm.

(G) Cell length of coleoptile as shown in **(E)**. The values are means ± SD of 20 to 30 cells per sample. The asterisks indicate significant difference compared with *gy1* (**$P < 0.01$, Student's *t* test).

(H) $GY1^{376G}$ expression inhibits the long mesocotyl and coleoptile phenotype in Kas with $GY1^{376T}$. Phenotype of etiolated seedlings from Kas and two transgenic lines transformed with $GY1^{376G}$ grown for 3 d after germination in darkness. Arrowheads indicate the coleoptilar nodes between the mesocotyl and coleoptile. The dCAPS marker was used to genotype GY1 and $GY1^{376T}$ by cleaving PCR products with *Fsp*I. dCAPS primers are listed in Supplemental Table 7. Bar = 10 mm.

(I) Coleoptile and mesocotyl length of etiolated seedlings from **(G)**. The values are means ± SD of 20 to 30 seedlings per sample. The asterisks indicate significant difference compared with Kas (**$P < 0.01$, Student's *t* test).

(J) JA contents in the shoots of etiolated seedlings from Kas (with $GY1^{376T}$) and two transgenic lines transformed with $GY1^{376G}$ grown for 3 d after germination in darkness. The values are means ± SD of three biological replicates (independent pools of tissue) per sample. The asterisks indicate significant difference compared with Kas (**$P < 0.01$, Student's *t* test).

GY1-Mediated JA Biosynthesis Inhibits Mesocotyl and Coleoptile Elongation

Our study demonstrates that GY1-mediated JA biosynthesis inhibits mesocotyl and coleoptile elongation in etiolated rice seedlings. The following pieces of evidence support our conclusion. First, the *gy1* mutant exhibited longer mesocotyls and longer coleoptiles than its wild-type Nip, and *GY1* could completely complement this phenotype (Figure 1). Second, JA content significantly decreased in the *gy1* mutant compared with that of Nip (Figure 3E). Third, the *cpm2/osaoc* mutant, which is also a JA biosynthesis pathway mutant, had a long mesocotyl and long coleoptile phenotype that resembled that of *gy1* (Supplemental Figure 6). Fourth, 1 μM MeJA could rescue the long mesocotyl and long coleoptile phenotype of the *gy1* mutant (Figures 3F and 3G). Fifth, a natural variation of 376T SNP in *GY1*, which resulted in an amino acid change from glycine to cysteine at position 126 of GY1, was identified from 3000 rice accessions. The presence of the 376T SNP was positively correlated with the long mesocotyl phenotype (Figure 8C; Supplemental Tables 3 and 4). Sixth, transforming the Kasalath variety harboring $GY1^{376T}$ with the wild-type $GY1^{376G}$ gene from Nip could largely suppress the long mesocotyl and long coleoptile phenotype of Kasalath (Figures 8H and 8I), and the transgenic lines had higher JA content than Kasalath (Figure 8J). Seventh, GY1 has PLA activity, and gy1 and $GY1^{376T}$ have much lower PLA activity than GY1. However, $GY1^{376T}$ has higher PLA activity than gy1. From all the evidence above, we conclude that the phospholipase GY1-mediated JA biosynthesis inhibits elongation of the mesocotyl and coleoptile in etiolated rice seedlings.

While mutation of *GY1* promotes mesocotyl and coleoptile elongation in the *gy1* mutant, the roots were not significantly affected (Supplemental Figure 1A), indicating the specificity of *GY1* function in seedlings. When analyzing the spatial expression of *GY1* in mesocotyls of Nip seedlings, the germinated Nip seeds were covered with soil to a 4 cm depth for three days, and under this condition, mesocotyl growth was promoted. In these mesocotyls, the expression of *GY1* turned out to be very low (Figure 2A), consistent with the negative relationship between *GY1* expression and mesocotyl elongation.

It should be noted that the etiolated seedlings of *gy1* exhibit both longer mesocotyls and longer coleoptiles than Nip. In a natural population, the 376T SNP of *GY1* is only associated with the long mesocotyl phenotype in etiolated seedlings, and the coleoptile length of seedlings was distributed over a large range due to background differences (Supplemental Table 4). Since there is no easy way to analyze the genetic effect of 376T SNP on the coleoptile phenotype among plants in a natural population by association analysis, we performed a complementation test in the Kasalath variety, which harbors $GY1^{376T}$, using the wild-type $GY1^{376G}$ from Nip. We found that $GY1^{376T}$ regulated the long coleoptile and the long mesocotyl phenotypes in etiolated seedlings.

This study reveals that GY1-mediated JA biosynthesis inhibits mesocotyl/coleoptile elongation of etiolated rice seedlings, affecting seedling emergence from soil cover. This finding is consistent with previous reports that show that JA inhibits seed germination in various plants, e.g., Arabidopsis, alfalfa (*Medicago sativa*), cornflower (*Centaurea cyanus*), rice, cress (*Lepidium sativum*), maize (*Zea mays*) (Wilen et al., 1994; Liu et al., 2015). However, the genes underlying the inhibition are still largely unknown. (9*S*,13*S*)-12-oxo-phytodienoic acid, a key metabolic intermediate during JA biosynthesis, acts synergistically with abscisic acid to inhibit germination in Arabidopsis (Dave et al., 2011). Arabidopsis DAD1, DGL, and DLAH are homologs of GY1 and exhibit PLA activity (Ishiguro et al., 2001; Hyun et al., 2008; Ellinger et al., 2010; Seo et al., 2011). DLAH-overexpressing transgenic seeds were tolerant to higher temperature and had higher germination percentages than did wild-type seeds (Seo et al., 2011). However, it is not clear whether Arabidopsis DAD1 and DGL are also involved in the seed germination process, although they both regulate floral development through JA synthesis (Ishiguro et al., 2001; Hyun et al., 2008).

In addition to its role in mesocotyl/coleoptile elongation and emergence from soil, GY1 affects floral development, as judged from the *gy1* mutant phenotype at maturity (Supplemental Figure 3). Floral development in plants is controlled by multiple signals and JA is one of them (Yuan and Zhang, 2015). The Arabidopsis homolog DAD1 and DGL-mediated JA biosynthesis regulates floral development (Ishiguro et al., 2001; Hyun et al., 2008). A *gy1* allelic mutant *extra glume1* (*eg1*) also exhibits an abnormal number of pistils and an extra glume-like organ in rice (Li et al., 2009; Zhang et al., 2016). The abnormal flower development of the *gy1* mutant may cause the reduction of yield-related traits (Supplemental Table 2). EG1/GY1 exhibited lipase activity in vitro (Zhang et al., 2016) and regulated lipid metabolism (Zhang et al., 2016) and JA biosynthesis (Cai et al., 2014) during rice floral development. Our analysis further showed that GY1 was an etioplast-localized PLA in etiolated seedlings (Figures 2B to 2D and 8B), preferred PC as a substrate (Figures 3A to 3D), and participated in JA biosynthesis to regulate skotomorphogenesis and floral development (Figures 3E and 3F; Supplemental Figure 3). Furthermore, the JA signaling repressor EG2/OsJAZ1 not only interacts with the JA receptor OsCOI1b to trigger OsJAZ1's degradation during spikelet development, but also interacts with OsMYC2 to repress an E-class gene *OsMADS1* that is crucial for spikelet development (Cai et al., 2014). These studies indicate that JA synthesis and signaling control the development of the inflorescence and flower.

Ethylene Signaling Inhibits JA Biosynthesis to Promote Mesocotyl/Coleoptile Elongation

In Arabidopsis, the ethylene pathway plays an important role in the growth of etiolated seedlings under soil environments (Zhong et al., 2014; Shi et al., 2016a, 2016b). Here, we find that the ethylene signaling pathway inhibits JA biosynthesis and eventually promotes mesocotyl and coleoptile elongation in etiolated rice seedlings to facilitate their emergence from soil. The following evidence supports this conclusion. First, ethylene production in rice seedlings increases along with the seed-sowing depth in soil (Figure 4E). By contrast, *GY1* expression and JA contents are reduced as the sowing depth increases (Figures 4C and 4D). Mesocotyl and coleoptile growth are promoted as the sowing depth increases (Figures 4A and 4B). Second, ethylene inhibits the expression of *GY1* and other genes in the JA biosynthesis pathway and further reduces the JA content in etiolated rice seedlings

(Figures 5A to 5C). Third, overexpression of ethylene signaling components MHZ7/OsEIN2 and OsEIL2 inhibits *GY1* expression (Figures 5D and 5E). Fourth, mutation of *MHZ7/OsEIN2* in the *mhz7/osein2* mutant disrupts the ethylene-mediated inhibition of *GY1* (Figure 5D). Fifth, OsEIL2 directly binds to the promoter region of *GY1*, as demonstrated by EMSA and ChIP-PCR assays, and represses *GY1* promoter activity in a tobacco leaf transient expression assay (Figures 5G to 5J). Sixth, double mutant analysis reveals that *GY1* acts downstream of *MHZ7/OsEIN2* to affect mesocotyl/coleoptile growth (Figures 6A and 6B). Seventh, JA application to the *MHZ7/OsEIN2*-overexpressing plants reduces mesocotyl/coleoptile elongation, suggesting that JA acts downstream of ethylene signaling for functional regulation (Figures 6C and 6D). All of this evidence demonstrates that ethylene interacts with JA to control mesocotyl/coleoptile elongation during the early emergence of rice seedlings.

It should be noted that although the *gy1* mutant already has a relatively long mesocotyl/coleoptile, ethylene treatment further promotes mesocotyl/coleoptile elongation (Supplemental Figures 1A to 1C). Additionally, it seems that the *gy1* mutant was more sensitive to ethylene than Nip during seedling emergence under soil-grown conditions. These facts suggest that, in addition to the inhibition of GY1-mediated JA biosynthesis, ethylene may regulate mesocotyl/coleoptile growth through other downstream mechanisms/factors. It has been reported that ethylene induces cell wall acidification and increases the extensibility of cells in *Rumex palustris* (Vreeburg et al., 2005). This is largely attributed to the acidic pH optimum for expansin activity (McQueen-Mason et al., 1992). Furthermore, ethylene regulates the stability of intracellular microtubules through WAVE-DAMPENED2-LIKE5 to mediate etiolated hypocotyl cell elongation in Arabidopsis (Sun et al., 2015). In addition, many loci have been identified that may regulate mesocotyl growth. Using a population of backcross inbred lines, five QTL have been found to control mesocotyl length in rice (Lee et al., 2012). *GY1* overlaps with one of these QTL. Through genome-wide association analysis of 270 rice accessions, Wu et al. (2015) identified 16 loci that control mesocotyl growth in rice seedlings grown in water or in sand. Recently, using the same genome-wide association analysis method, Lu et al. (2016) analyzed 469 rice accessions and discovered 23 loci involved in the regulation of mesocotyl/shoot growth. Dissection of all these loci may reveal the complete mechanisms involved in mesocotyl regulation.

When analyzing the role of ethylene signaling in *GY1* inhibition, *MHZ7/OsEIN2* appeared to be fully required for ethylene-mediated *GY1* inhibition, whereas knocking down of *OsEIL2* seemed not to significantly affect the ethylene-induced *GY1* inhibition in shoots (Figures 5D and 5E). However, in our previous study, we found that coleoptile growth of the *OsEIL2*-RNAi seedlings was insensitive to ethylene (Yang et al., 2015b). The discrepancy then existed that the same *OsEIL2*-RNAi plants are insensitive to ethylene with respect to ethylene-promoted coleoptile elongation but sensitive to ethylene with respect to ethylene-induced *GY1* inhibition. This phenomenon may be explained by the fact that although *OsEIL2* expression was reduced in the *OsEIL2*-RNAi plants, significant levels of residual *OsEIL2* transcripts remained (Yang et al., 2015b) and that the resulting OsEIL2 activity may be enough to inhibit *GY1* expression, but not reach the threshold to promote coleoptile elongation in response to ethylene. Alternatively, differential sensitivity to ethylene may be one of the reasons for different responses. Other explanations/possibilities cannot be excluded.

Natural Variation of 376T SNP in *GY1* Correlates with Mesocotyl Elongation in Rice Accessions

Although *GY1* mutation-mediated mesocotyl elongation may facilitate seedling emergence from soil, this mutation affects flowering development and yield-related traits (Supplemental Table 2). Such a defect prevents the use of the *GY1* mutation in breeding efforts. We thus examined whether elite natural alleles are present in different rice accessions. After analyzing the re-sequencing data of 3000 rice accessions (Li et al., 2014), only one natural variant of *GY1* was discovered, which harbors a 376T instead of the original 376G present in Nip. This elite $GY1^{376T}$ allele is positively correlated with mesocotyl elongation in rice. Introducing a wild-type $GY1^{376G}$ into the Kasalath accession, which harbors the $GY1^{376T}$ and has a long mesocotyl and coleoptile phenotype, increases the JA content and largely inhibits mesocotyl and coleoptile growth, indicating that GY1 may be the major factor regulating mesocotyl and coleoptile growth. Indeed, *GY1* is located within a major QTL for mesocotyl regulation, which was identified from backcross inbred lines developed from Kasalath and Nipponbare (Lee et al., 2012). From these analyses, we identified an elite natural variation of $GY1^{376T}$, which promotes mesocotyl elongation and has no yield penalty. This allele may be introduced into accessions lacking it by breeding to produce new rice cultivars, and these cultivars should be suitable for growing in dry land due to their high emergence rate.

The 141 rice varieties harboring 376T in *GY1* mainly belong to the subgroups Aus/boro, Indica type, and Aromatic type (basmati/sandri type) (Supplemental Table 3). These accessions mainly originated from Asian countries with tropical monsoon climates, including Bangladesh, India, Pakistan, and Nepal. Long-term cultivation and domestication may have selected the $GY1^{376T}$ variant, which enables the plant to withstand such climates. It should be noted that only a small proportion of Japonica rice has this allele (Supplemental Table 3). The elite allele should be introduced into Japonica varieties to test the effect of this allele on mesocotyl and coleoptile elongation and rice adaptation to dry upland.

Taken together, our study reveals that ethylene-inhibited GY1-mediated JA biosynthesis promotes mesocotyl/coleoptile elongation in etiolated rice seedlings. We further associate an elite natural allele $GY1^{376T}$ with mesocotyl elongation in different rice accessions. Our study provides insight into the mechanism underlying mesocotyl/coleoptile elongation, and this knowledge should facilitate the practical use of the elite allele in rice breeding programs.

METHODS

Plant Materials and Growth Conditions

The *gy1* mutant used in this study was in the *Japonica* background (*Oryza sativa* cv Nipponbare) and isolated from a T-DNA insertion population (Ma et al., 2013). The *cpm2* mutant (*O. sativa* cv Nihonmasari) was kindly provided by Moritoshi Iino (Graduate School of Science, Osaka City

University). The seeds of various rice accessions were kindly provided by Zhi-Kang Li (Institute of Crop Sciences/National Key Facilities for Crop Gene Resources and Genetic Improvement, Chinese Academy of Agricultural Sciences). For material propagation, crossing, and investigation of agronomic traits, rice plants were cultivated at the Experimental Station of the Institute of Genetics and Developmental Biology in Beijing during the natural growing seasons from May to October.

Seeds were germinated in water at 37°C in darkness for 2 d as previously described (Ma et al., 2013). To measure the mesocotyls and coleoptiles, the germinated seeds were incubated in darkness at 28°C and grown for 3 to 4 d as indicated in each experiment. For ethylene treatments, the germinated seeds were incubated in darkness at 28°C for 2 to 3 d and then treated with 10 ppm ethylene (Ma et al., 2013). For the seedling emergence experiment, germinated seeds were sown at a 2-cm depth in pots containing soil. The pots were placed under 20,000 lux white fluorescent light (14 h light/10 h dark) at 28°C and with 75% relative humidity.

Map-Based Cloning

To determine the *GY1* locus, the mutant *gy1* was crossed with an *Indica* variety, cv TN1. The genomic DNA of etiolated seedlings from members of the F2 population exhibiting the mutant phenotype was extracted using the SDS method (Dellaporta et al., 1983). For rough mapping, a DNA pool generated from 15 individuals with the mutant phenotype was used. A total of 927 individuals with the mutant phenotype selected from the F2 population were used for fine mapping. The insertion-deletion (Idl) markers and simple sequence repeat markers were the same as previously described (Ma et al., 2013). The *GY1* locus was mapped to chromosome 1 between Idl1-39.15 (5′-TTGTTGTGCATACTACAGCTAG-3′ and 5′-CTAAGCTAATTTCAAGACTGCC-3′) and Idl1-39.20 (5′-TGATGCAGTCAACTGGCTTG-3′ and 5′-ACAATCAACGGGTCGACATC-3′), which is a 48-kb region containing three genes. The candidate gene was finally determined by sequencing all three genes in this region. The *gy1* mutation was confirmed via the dCAPS (derived cleaved amplified polymorphic sequence) marker. The restriction enzyme site was introduced by reverse primer 5′-acgagacgagcacgtAGCGC-3′ (519th nucleotide). When amplifying *GY1* (*GY1*^{518G}) and *gy1* (*GY1*^{518A}), we could generate the *Aor*51HI restriction site (AGCGCT) in the product of *gy1* but not in the product of GY1 (see Supplemental Table 7). The PCR product was then cleaved by *Aor*51HI, and the resulting product of *gy1* was shorter than that of *GY1*.

Vector Construction and Rice Transformation

For construction of the complementation plasmid *pC-GY1*, a fragment of *GY1* was inserted into the pCAMBIA2300 vector with *Sma*I and *Sse*8387 I sites to generate *pC-GY1*. This insertion fragment of 4806 bp was a *GY1* genomic sequence containing the 1308-bp *GY1* coding sequence, the 2022-bp promoter sequence upstream of the ATG start codon of *GY1*, and the 1476-bp sequence downstream of the TGA stop codon of *GY1*.

For subcellular localization, the pBI-*GY1-GFP* plasmid was produced. The coding sequence of *GY1* was digested with *Bam*HI/*Hin*dIII and cloned into the pBI221-*GFP* vector that had also been digested with *Bam*HI/*Hin*dIII. The GFP coding sequence was fused in frame to the 3′ end of *GY1*.

For the transcriptional regulation assay in tobacco leaves, the coding sequence (2500 bp) of *OsEIL2* was inserted into the pCAMBIA2300-*35S-ocs* vector to generate the effector plasmid *35S*:*OsEIL2*. The *GY1* promoter fragment (2022 bp) upstream from the ATG start codon of *GY1* was cloned into pGWB435 (Invitrogen) to generate the reporter plasmid *pGY1*:*LUC*.

The primers used to generate the constructs are listed in Supplemental Table 5.

The *pC-GY1* plasmid was transfected into *Agrobacterium tumefaciens* strain EHA105 through electroporation, and the strain harboring the construct was then transformed into the *gy1* mutant or the Kasalath variety for complementation tests. Rice transformation was performed as described previously (Wuriyanghan et al., 2009). The complemented *gy1* mutant and Kasalath variety were genotyped by dCAPS marker analysis using the primers listed in Supplemental Table 7. The PCR products from *gy1* and Kasalath were digested with the restriction enzymes *Aor*51HI and *Fsp*I, respectively.

Subcellular Localization Assays

To determine the subcellular localization of GY1, the pBI-*GY1-GFP* construct was transformed into rice protoplasts and Arabidopsis protoplasts by polyethylene glycol-mediated transfection as described (Bart et al., 2006; Yang et al., 2015b). After 12 to 16 h of incubation at 28°C under darkness, GFP fluorescence was observed with a confocal laser scanning microscope (Leica TCS SP5).

Phylogenetic Analysis

The protein sequences of GY1 homologs in *Arabidopsis thaliana* and rice were downloaded from Phytozome v.11 and then aligned with ClustalX v2.1 (Supplemental Data Set 1). The neighbor-joining method was used to construct a phylogenetic tree with 1000 replicates in Phylip v3.69. The tree was viewed in MEGA v.7.

Lipid Analysis

Lipid extractions for rice tissues were performed using a modified version of the Bligh and Dyer's protocol as previously described (Lam et al., 2014b). Extracted organic fractions were pooled and dried in miVac (Genevac). Samples were stored at −80°C until further analysis.

Polar lipids were analyzed using an Agilent 1260 HPLC system coupled with a triple quadrupole/ion trap mass spectrometer (5500Qtrap; SCIEX) as described previously (Lam et al., 2014a). Individual lipid species were quantified by referencing to spiked internal standards. Galactolipids (MGDGs and DGDGs) were separated using a Phenomenex Kinetex 2.6μ-C18 column as previously described (Cheong et al., 2014).

Protein Expression and PLA Activity Assay

The codons of *GY1*, *gy1* (*GY1*^{518A}), and *GY1*^{376T} were optimized for expression in *Escherichia coli* (http://www.jcat.de) and synthesized. The fragments were cloned into pET-SUMO (Invitrogen) by TA cloning. The His6-SUMO-tagged fusion proteins were expressed in *E. coli* BL21 (DE3), purified using Ni-NTA (Novagen), and eluted with buffer containing 25 mM Tris-HCl (pH 7.4), 150 mM NaCl, and 250 mM imidazole. Imidazole in protein solution was removed via desalting columns (Thermo Scientific) before activity analysis.

The PLA activity was determined as described (Ishiguro et al., 2001) with some modifications. Dye-labeled 1-BODIPY FL C11-2-BODIPY FL C11-PC (Molecular Probes) was used as substrate for measuring PLA activity. In brief, 30 μL of 2 mM PLA substrate was mixed with 30 μL of 10 mM dioleoyl-phosphatidylcholine and 30 μL of 10 mM dioleoyl-phosphatidylglycerol in 5 mL reaction buffer (50 mM Tris-HCl, 140 mM NaCl, and 1 mM $CaCl_2$, pH 7.4) to generate substrate-liposome mix. Then, ~20 μg purified proteins and 50 μL substrate-liposome mix in total 100 μL reaction buffer were incubated at room temperature for 30 min. The fluorescence was measured at multiple time points to monitor the kinetics using a microplate reader equipped for excitation at 450 nm and fluorescence emission at 515 nm. The known activity unit of Lecitase Ultra (Novozymes) was used as a positive control to obtain the standard curve. SUMO protein was used as no-PLA control to correct for background fluorescence.

Measurement of JA Content and Ethylene Production

For JA measurement in water-grown seedlings, 2-d-old etiolated seedlings of Nip and *gy1* were treated with or without 10 ppm ethylene for 24 h, and

the shoots, which contain the coleoptiles and the true leaves, were harvested. Each sample was ground in liquid nitrogen, weighed (~200 mg for each sample), and stored at −80°C until extraction.

For JA measurement during seedling emergence from soil, different volumes of 0.6% Agar A were poured into 45-mL vials to generate supporting matrix with different heights. Germinated seeds of Nip were then placed on the surface of solidified 0.6% Agar A and covered with different depths of sterilized soil (0, 1, and 2 cm) with water saturation. Finally, the agar matrix (0 cm), and the agar matrix plus the soil (1 and 2 cm) have the same height. The 3-d-old seedlings were ground in liquid nitrogen, weighed (~200 mg for each sample), and stored at −80°C until extraction.

JA was purified and measured as previously described with some changes in detection conditions (Fu et al., 2012).

For ethylene production in water-grown seedlings, the germinated seeds were cultured in darkness in a 45-mL uncapped vial for 7 d at 28°C, and then the vials were sealed with a rubber cap for 15 h. After this treatment, ethylene emission was measured.

For ethylene production during seedling emergence from soil, a similar culturing method was used as was used to measure JA content during seedling emergence from soil in uncapped vials, and then the vials were sealed with a rubber cap for 20 h. After the treatment, ethylene emission was measured.

Ethylene production was determined by gas chromatography (GC2014; Shimadzu) using an instrument equipped with a flame ionization detector.

JA and ethylene measurements were repeated three times, and each sample had three biological and technical replicates. The averages and standard deviations are shown.

MeJA Treatment to Rescue the Mutant Phenotype

To rescue the long mesocotyl and coleoptile phenotype of *gy1* with MeJA (Sigma-Aldrich), 0.01, 0.1, 1, and 10 μM MeJA were used to obtain a dose-response curve for the Nip coleoptile. The MeJA solutions were dissolved in ethanol, and equivalent volumes of ethanol were added for the mock treatment as for the control. A concentration of 1 μM MeJA was used to rescue the mutant phenotype. Germinated seeds were placed on stainless steel sieves in 5.5-liter air-tight plastic boxes, and 1.5 liters of MeJA solution and mock solution were added to these plastic boxes separately. After growth for 3 d at 28°C in darkness, the lengths of the coleoptiles and mesocotyls were measured.

Gene Expression Analysis by qPCR

Total RNA was extracted with TRIzol reagent (Invitrogen). Using a Turbo DNA-free Kit (Invitrogen) and a cDNA synthesis kit (TaKaRa), the acquired cDNA samples were used to perform qPCR with the LightCycler 480II (Roche). *OsActin2* was used as the internal control. The primers used are listed in Supplemental Table 5.

ChIP-PCR Analysis

For the ChIP assay, the *OsEIL2-GFP* cassette was cloned into the pCAMBIA2300-*35S-ocs* vector to generate the *35S*:*OsEIL2*:*GFP* plasmid, which was then transformed into Nip by Agrobacterium-mediated transfection. Shoots (1.5 g) of 3-d-old etiolated seedlings of the Nip and *OsEIL2-GFP* line were prepared for ChIP assays. In brief, each sample was cross-linked in 37 mL cross-link buffer (1% formaldehyde, 0.1 M sucrose, 10 mM sodium phosphate, and 50 mM NaCl, pH 8.0) under a vacuum in an exicator for 30 min, and then 2.5 mL of 2 M glycine was added to quench cross-linking under a vacuum. Chromatin was isolated and resuspended in 75 μL lysis buffer (1% SDS, 50 mM Tris-HCl, pH 8.0, and 10 mM EDTA). Then, 625 μL of dilution buffer (1.1% Triton X-100, 50 mM Tris-HCl, pH 8.0, 167 mM NaCl, 1.2 mM EDTA, 1 mM PMSF, and one tablet of protease inhibitor cocktail) was added and the sample was sonicated with a Bioruptor for 10 min on ice (10 s on/45 s off cycles). The chromatin sample was then incubated at 4°C overnight with GFP antibody (A6455; Invitrogen). Immunoprecipitated complexes were collected using magnetic protein G/A beads (Invitrogen) and washed with low salt (150 mM NaCl, 0.1% SDS, 1% Triton X-100, 2 mM EDTA, and 20 mM Tris-HCl, pH 8.0), high salt (500 mM NaCl, 0.1% SDS, 1% Triton X-100, 2 mM EDTA, and 20 mM Tris-HCl, pH 8.0), and LiCl washing (0.25 M LiCl, 1% Nonidet P-40, 1% sodium deoxycholate, 1 mM EDTA, and 10 mM Tris-HCl, pH 8.0) buffer successively. The immunoprecipitated complexes were incubated in lysis buffer at 65°C for 4 h. DNA was recovered with a QIAquick PCR purification kit (Qiagen) and analyzed by real-time PCR using primers as described (Supplemental Table 5). The chromatin isolated before precipitation was used as an input control, and the chromatin precipitated without antibody was used as a negative control. The "% input" value of each ChIP-PCR fragment was calculated first by normalizing the fragment amount against the input value and then by normalizing the value from the transgenic plants against the value from the control plants.

Transcriptional Regulatory Activity of OsEIL2 on the *GY1* Promoter in Tobacco Leaves

The reporter plasmid (*pGY1:LUC*) and the effector plasmids (*35S*:*OsEIL2*) were transformed into Agrobacterium strain EHA105. The strains were later resuspended in infiltration buffer (10 mM MES, 0.2 mM acetosyringone, and 10 mM $MgCl_2$) to an ultimate concentration of optical density (600 nm = 1). Equal amounts of different combined suspensions were infiltrated into the young leaves of 5-week-old tobacco (*Nicotiana tabacum*) plants with syringes without needles. After growth in darkness for 12 h, the infiltrated plants were cultivated under 16 h light/8 h darkness for 48 h at 24°C. Before observation, the leaves were sprayed with 100 mM luciferin (Promega) and placed in darkness for 5 min. A low-light cooled CCD imaging apparatus (iXon; Andor Technology) was then used to observe the LUC activity of each experiment.

EMSA

Plasmid construction and protein purification of OsEIL2 (amino acids 1–354) followed previous descriptions (Yang et al., 2015b). Single-stranded complementary oligonucleotide fragments containing the EIN3 binding elements from the *GY1* promoter were synthesized (Invitrogen) and biotinylated using the Biotin 3′-end DNA Labeling Kit (Thermo Fisher Scientific). Biotin end-labeled and unlabeled oligonucleotide pairs were annealed to obtain double-stranded biotin-labeled and unlabeled probes by mixing equal amounts of each single-stranded complementary oligonucleotide fragment, incubating the fragments at 95°C for 5 min, and cooling them down to room temperature slowly overnight. The EMSA reaction solutions were prepared using the LightShift Chemiluminescent EMSA Kit (Thermo Fisher Scientific). After the reactions, the protein-probe mixtures were separated on a 6% nondenaturing neutral polyacrylamide gel in 0.5× TBE and transferred to a nylon membrane (GE). After UV light cross-linking, the DNA on the membrane was detected with the Chemiluminescent Nucleic Acid Detection Module (Thermo Fisher Scientific).

The oligonucleotide sequences used are listed in Supplemental Table 6.

RNA-Seq Library Preparation and Bioinformatics Analysis

Seeds of Nip and the *gy1* mutant were germinated at 37°C in darkness for 2 d as previously described (Ma et al., 2013). The germinated seeds were sown at a 4-cm depth in pots containing soil, and the seedlings were grown under 14 h light/10 h dark at 28°C for 3 d. The etiolated seedlings were removed from the pots, and the mesocotyls were harvested. The total RNA was extracted with CTAB buffer according to previous descriptions (Fu et al., 2004; Yin et al., 2016). The library preparation and bioinformatics analysis followed previous descriptions (Yang et al., 2015b).

Agronomic Trait Analysis

After harvest, Nip and *gy1* were evaluated for agronomic traits and 25 plants from each material were used for measurements. For each plant, plant height and yield-related traits were measured. Seed-setting rate was calculated as filled grain number/total grain number. Other traits were also measured, and the average from 25 plants was provided for each genotype in Supplemental Table 2. All the data were analyzed by one-way ANOVA (LSD and S-N-K) for test groups with SPSS 18.0.

Accession Numbers

Sequence data from this article can be found in the GenBank/EMBL data libraries under the following accession numbers: LOC_Os01g67430 (*GY1*), LOC_Os02g10120 (*OsLOX*), LOC_Os03g55800 (*OsAOS1*), LOC_Os03g12500 (*OsAOS2*), LOC_Os03g32314 (*OsAOC*), LOC_Os08g35740 (*OsOPR7*), LOC_Os01g60770 (*OsEXPA2*), LOC_Os05g39990 (*OsEXPA4*), LOC_Os10g40730 (*OsEXPB4*), LOC_Os10g40700 (*OsEXPB6*), LOC_Os02g44108 (*OsEXPB11*), LOC_Os03g04020 (*OsEXPLA1*), and LOC_Os10g36650 (*OsActin2*).

Supplemental Data

Supplemental Figure 1. Ethylene Response and Ethylene Production of *gy1*.

Supplemental Figure 2. Emergence Rate of *gy1* Compared with the Nip Control.

Supplemental Figure 3. Phenotype of *gy1* and *GY1*-Complemental Plants at Maturity Stage.

Supplemental Figure 4. GY1 Subcellular Localization in Arabidopsis Protoplasts.

Supplemental Figure 5. Phylogenetic Analysis of GY1 and Its Homologs.

Supplemental Figure 6. Phenotype Analysis of Another JA Biosynthesis Mutant.

Supplemental Figure 7. MeJA Dose-Response Curve for Coleoptile Length of Etiolated Seedlings.

Supplemental Figure 8. Ethylene Inhibits JA Level and *GY1* Expression in Shoots of Deetiolated Seedlings.

Supplemental Figure 9. Identification of Differentially Expressed Genes and GO Enrichment Analysis.

Supplemental Figure 10. Phenotype of Etiolated Seedlings from Different Rice Accessions.

Supplemental Table 1. Dominant/Recessive Analysis of Mutant Phenotype.

Supplemental Table 2. Agronomic Traits of Field-Grown Nip and *gy1* in 2012 and 2014.

Supplemental Table 3. The Number of Allelic Variation of GY1 in Rice Accessions.

Supplemental Table 4. The Mesocotyl and Coleoptile Length in Different Genotypes of *GY1* in Etiolated Seedlings of Different Varieties.

Supplemental Table 5. Primers Used for Gene Expression Analysis and Vector Construction.

Supplemental Table 6. Oligonucleotides Used for EMSA.

Supplemental Table 7. Primers Used for *gy1* Allelic Mutant Analysis.

Supplemental Data Set 1. Alignments Used to Generate the Phylogeny Presented in Supplemental Figure 5.

ACKNOWLEDGMENTS

This work was supported by the 973 project (2015CB755702), the National Natural Science Foundation of China (31530004, 31670274, and 31600980), the Transgenic Research Projects (2016ZX08009003-002), the Postdoctoral Research Fellowship (2015M581200 to C.-C.Y.), and the State Key Lab of Plant Genomics. We thank Shuang Fang and Jin-Fang Chu (National Centre for Plant Gene Research [Beijing], Institute of Genetics and Developmental Biology, Chinese Academy of Sciences, Beijing) for determining the JA contents. We also thank Sin-Man Lam and Guang-Hou Shui (Institute of Genetics and Developmental Biology, Chinese Academy of Sciences, Beijing) for determining the lipid contents.

AUTHOR CONTRIBUTIONS

Q.X., B.M., J.-S.Z., and S.-Y.C. conceived and designed the experiments. Q.X. performed the experiments. B.M. isolated the *gy1* mutant. X.L. performed the bioinformatics analysis and some of the experiments. S.-J.H. carried out the rice transformation. Y.-H.H., C.Y., C.-C.Y., H.Z., Y.Z., and W.-K.Z. prepared some of the materials. W.-S.W. and Z.-K.L. provided rice variety seeds. Q.X., J.-S.Z., and B.M. wrote the article.

Received January 3, 2017; revised March 27, 2017; accepted May 2, 2017; published May 2, 2017.

REFERENCES

Alonso, J.M., Hirayama, T., Roman, G., Nourizadeh, S., and Ecker, J.R. (1999). EIN2, a bifunctional transducer of ethylene and stress responses in *Arabidopsis.* Science **284:** 2148–2152.

Bannenberg, G., Martínez, M., Hamberg, M., and Castresana, C. (2009). Diversity of the enzymatic activity in the lipoxygenase gene family of *Arabidopsis thaliana.* Lipids **44:** 85–95.

Bart, R., Chern, M., Park, C.J., Bartley, L., and Ronald, P.C. (2006). A novel system for gene silencing using siRNAs in rice leaf and stem-derived protoplasts. Plant Methods **2:** 13.

Biswas, K.K., Neumann, R., Haga, K., Yatoh, O., and Iino, M. (2003). Photomorphogenesis of rice seedlings: a mutant impaired in phytochrome-mediated inhibition of coleoptile growth. Plant Cell Physiol. **44:** 242–254.

Bleecker, A.B., and Kende, H. (2000). Ethylene: a gaseous signal molecule in plants. Annu. Rev. Cell Dev. Biol. **16:** 1–18.

Boutrot, F., Segonzac, C., Chang, K.N., Qiao, H., Ecker, J.R., Zipfel, C., and Rathjen, J.P. (2010). Direct transcriptional control of the *Arabidopsis* immune receptor FLS2 by the ethylene-dependent transcription factors EIN3 and EIL1. Proc. Natl. Acad. Sci. USA **107:** 14502–14507.

Cai, Q., Yuan, Z., Chen, M., Yin, C., Luo, Z., Zhao, X., Liang, W., Hu, J., and Zhang, D. (2014). Jasmonic acid regulates spikelet development in rice. Nat. Commun. **5:** 3476.

Chao, Q., Rothenberg, M., Solano, R., Roman, G., Terzaghi, W., and Ecker, J.R. (1997). Activation of the ethylene gas response pathway in *Arabidopsis* by the nuclear protein ETHYLENE-INSENSITIVE3 and related proteins. Cell **89:** 1133–1144.

Chauvin, A., Caldelari, D., Wolfender, J.L., and Farmer, E.E. (2013). Four 13-lipoxygenases contribute to rapid jasmonate synthesis in wounded *Arabidopsis thaliana* leaves: a role for lipoxygenase 6 in responses to long-distance wound signals. New Phytol. **197:** 566–575.

Cheong, W.F., Wenk, M.R., and Shui, G. (2014). Comprehensive analysis of lipid composition in crude palm oil using multiple lipidomic approaches. J. Genet. Genomics **41:** 293–304.

Cho, H.T., and Cosgrove, D.J. (2000). Altered expression of expansin modulates leaf growth and pedicel abscission in *Arabidopsis thaliana.* Proc. Natl. Acad. Sci. USA **97:** 9783–9788.

Choi, D., Lee, Y., Cho, H.T., and Kende, H. (2003). Regulation of expansin gene expression affects growth and development in transgenic rice plants. Plant Cell **15:** 1386–1398.

Dave, A., Hernández, M.L., He, Z., Andriotis, V.M.E., Vaistij, F.E., Larson, T.R., and Graham, I.A. (2011). 12-Oxo-phytodienoic acid accumulation during seed development represses seed germination in *Arabidopsis.* Plant Cell **23:** 583–599.

Dellaporta, S.L., Wood, J., and Hicks, J.B. (1983). A plant DNA minipreparation: Version II. Plant Mol. Biol. Report. **1:** 19–21.

Dilday, R.H., Mgonja, M.A., Amonsilpa, S.A., Collins, F.C., and Wells, B.R. (1990). Plant height vs. mesocotyl and coleoptile elongation in rice: linkage or pleiotropism. Crop Sci. **30:** 815–818.

Eastmond, P.J., and Graham, I.A. (2000). The multifunctional protein AtMFP2 is co-ordinately expressed with other genes of fatty acid beta-oxidation during seed germination in *Arabidopsis thaliana* (L.) Heynh. Biochem. Soc. Trans. **28:** 95–99.

Eastmond, P.J., Hooks, M.A., Williams, D., Lange, P., Bechtold, N., Sarrobert, C., Nussaume, L., and Graham, I.A. (2000). Promoter trapping of a novel medium-chain acyl-CoA oxidase, which is induced transcriptionally during *Arabidopsis* seed germination. J. Biol. Chem. **275:** 34375–34381.

Ellinger, D., Stingl, N., Kubigsteltig, I.I., Bals, T., Juenger, M., Pollmann, S., Berger, S., Schuenemann, D., and Mueller, M.J. (2010). DONGLE and DEFECTIVE IN ANTHER DEHISCENCE1 lipases are not essential for wound- and pathogen-induced jasmonate biosynthesis: redundant lipases contribute to jasmonate formation. Plant Physiol. **153:** 114–127.

Feussner, I., and Wasternack, C. (2002). The lipoxygenase pathway. Annu. Rev. Plant Biol. **53:** 275–297.

Fu, J., Chu, J., Sun, X., Wang, J., and Yan, C. (2012). Simple, rapid, and simultaneous assay of multiple carboxyl containing phytohormones in wounded tomatoes by UPLC-MS/MS using single SPE purification and isotope dilution. Anal. Sci. **28:** 1081–1087.

Fu, X.H., Deng, S.L., Su, G.H., and Shi, S.H. (2004). Isolating high-quality RNA from mangroves without liquid nitrogen. Plant Mol. Biol. Report. **22:** 197.

Guo, H., and Ecker, J.R. (2004). The ethylene signaling pathway: new insights. Curr. Opin. Plant Biol. **7:** 40–49.

Hayashi, H., De Bellis, L., Ciurli, A., Kondo, M., Hayashi, M., and Nishimura, M. (1999). A novel acyl-CoA oxidase that can oxidize short-chain acyl-CoA in plant peroxisomes. J. Biol. Chem. **274:** 12715–12721.

Helms, R.S., Dilday, R.H., Mgonja, M.A., and Amonsilpa, S. (1989). Genetic and plant growth regulator manipulation of rice (*Oryza sativa* L.) mesocotyl and coleoptile lengths. Proc. Ark. Acad. Sci **43:** 42–45.

Hu, Z., Yan, H., Yang, J., Yamaguchi, S., Maekawa, M., Takamure, I., Tsutsumi, N., Kyozuka, J., and Nakazono, M. (2010). Strigolactones negatively regulate mesocotyl elongation in rice during germination and growth in darkness. Plant Cell Physiol. **51:** 1136–1142.

Hu, Z., Yamauchi, T., Yang, J., Jikumaru, Y., Tsuchida-Mayama, T., Ichikawa, H., Takamure, I., Nagamura, Y., Tsutsumi, N., Yamaguchi, S., Kyozuka, J., and Nakazono, M. (2014). Strigolactone and cytokinin act antagonistically in regulating rice mesocotyl elongation in darkness. Plant Cell Physiol. **55:** 30–41.

Hua, J., and Meyerowitz, E.M. (1998). Ethylene responses are negatively regulated by a receptor gene family in *Arabidopsis thaliana.* Cell **94:** 261–271.

Huang, J., Takano, T., and Akita, S. (2000). Expression of α-expansin genes in young seedlings of rice (*Oryza sativa* L.). Planta **211:** 467–473.

Hyun, Y., et al. (2008). Cooperation and functional diversification of two closely related galactolipase genes for jasmonate biosynthesis. Dev. Cell **14:** 183–192.

Ishiguro, S., Kawai-Oda, A., Ueda, J., Nishida, I., and Okada, K. (2001). The *DEFECTIVE IN ANTHER DEHISCENCE1* gene encodes a novel phospholipase A1 catalyzing the initial step of jasmonic acid biosynthesis, which synchronizes pollen maturation, anther dehiscence, and flower opening in *Arabidopsis*. Plant Cell **13:** 2191–2209.

Ju, C., et al. (2012). CTR1 phosphorylates the central regulator EIN2 to control ethylene hormone signaling from the ER membrane to the nucleus in *Arabidopsis.* Proc. Natl. Acad. Sci. USA **109:** 19486–19491.

Kieber, J.J., Rothenberg, M., Roman, G., Feldmann, K.A., and Ecker, J.R. (1993). *CTR1*, a negative regulator of the ethylene response pathway in *Arabidopsis*, encodes a member of the raf family of protein kinases. Cell **72:** 427–441.

Lam, S.M., Tong, L., Duan, X., Petznick, A., Wenk, M.R., and Shui, G. (2014a). Extensive characterization of human tear fluid collected using different techniques unravels the presence of novel lipid amphiphiles. J. Lipid Res. **55:** 289–298.

Lam, S.M., Wang, Y., Duan, X., Wenk, M.R., Kalaria, R.N., Chen, C.P., Lai, M.K.P., and Shui, G. (2014b). Brain lipidomes of subcortical ischemic vascular dementia and mixed dementia. Neurobiol. Aging **35:** 2369–2381.

Lee, H.S., Sasaki, K., Higashitani, A., Ahn, S.N., and Sato, T. (2012). Mapping and characterization of quantitative trait loci for mesocotyl elongation in rice (*Oryza sativa* L.). Rice (N. Y.) **5:** 13.

Li, H., Xue, D., Gao, Z., Yan, M., Xu, W., Xing, Z., Huang, D., Qian, Q., and Xue, Y. (2009). A putative lipase gene *EXTRA GLUME1* regulates both empty-glume fate and spikelet development in rice. Plant J. **57:** 593–605.

Li, W., Ma, M., Feng, Y., Li, H., Wang, Y., Ma, Y., Li, M., An, F., and Guo, H. (2015). EIN2-directed translational regulation of ethylene signaling in *Arabidopsis.* Cell **163:** 670–683.

Li, Y., Jones, L., and McQueen-Mason, S. (2003). Expansins and cell growth. Curr. Opin. Plant Biol. **6:** 603–610.

Li, Z.K., et al.; 3,000 Rice Genomes Project (2014) The 3,000 rice genomes project. Gigascience **3:** 7.

Liu, Z., Zhang, S., Sun, N., Liu, H., Zhao, Y., Liang, Y., Zhang, L., and Han, Y. (2015). Functional diversity of jasmonates in rice. Rice (NY) **8:** 42.

Lorenzo, O., Piqueras, R., Sánchez-Serrano, J.J., and Solano, R. (2003). ETHYLENE RESPONSE FACTOR1 integrates signals from ethylene and jasmonate pathways in plant defense. Plant Cell **15:** 165–178.

Lu, Q., Zhang, M., Niu, X., Wang, C., Xu, Q., Feng, Y., Wang, S., Yuan, X., Yu, H., Wang, Y., and Wei, X. (2016). Uncovering novel loci for mesocotyl elongation and shoot length in indica rice through genome-wide association mapping. Planta **243:** 645–657.

Ma, B., Chen, S.Y., and Zhang, J.S. (2010). Ethylene signaling in rice. Chin. Sci. Bull. **55:** 2204–2210.

Ma, B., Yin, C.C., He, S.J., Lu, X., Zhang, W.K., Lu, T.G., Chen, S.Y., and Zhang, J.S. (2014). Ethylene-induced inhibition of root growth requires abscisic acid function in rice (*Oryza sativa* L.) seedlings. PLoS Genet. **10:** e1004701.

Ma, B., et al. (2013). Identification of rice ethylene-response mutants and characterization of *MHZ7/OsEIN2* in distinct ethylene response and yield trait regulation. Mol. Plant **6:** 1830–1848.

McQueen-Mason, S., Durachko, D.M., and Cosgrove, D.J. (1992). Two endogenous proteins that induce cell wall extension in plants. Plant Cell **4:** 1425–1433.

Penninckx, I.A.M.A., Thomma, B.P.H.J., Buchala, A., Métraux, J.P., and Broekaert, W.F. (1998). Concomitant activation of jasmonate and ethylene response pathways is required for induction of a plant defensin gene in *Arabidopsis.* Plant Cell **10:** 2103–2113.

Qiao, H., Shen, Z., Huang, S.S.C., Schmitz, R.J., Urich, M.A., Briggs, S.P., and Ecker, J.R. (2012). Processing and subcellular trafficking of ER-tethered EIN2 control response to ethylene gas. Science **338:** 390–393.

Riemann, M., Riemann, M., and Takano, M. (2008). Rice JASMONATE RESISTANT 1 is involved in phytochrome and jasmonate signalling. Plant Cell Environ. **31:** 783–792.

Riemann, M., Muller, A., Korte, A., Furuya, M., Weiler, E.W., and Nick, P. (2003). Impaired induction of the jasmonate pathway in the rice mutant hebiba. Plant Physiol. **133:** 1820–1830.

Riemann, M., et al. (2013). Identification of rice *Allene Oxide Cyclase* mutants and the function of jasmonate for defence against *Magnaporthe oryzae.* Plant J. **74:** 226–238.

Rzewuski, G., and Sauter, M. (2008). Ethylene biosynthesis and signaling in rice. Plant Sci. **175:** 32–42.

Schaller, A., and Stintzi, A. (2009). Enzymes in jasmonate biosynthesis - structure, function, regulation. Phytochemistry **70:** 1532–1538.

Schaller, F., Biesgen, C., Müssig, C., Altmann, T., and Weiler, E.W. (2000). 12-Oxophytodienoate reductase 3 (OPR3) is the isoenzyme involved in jasmonate biosynthesis. Planta **210:** 979–984.

Seo, Y.S., Kim, E.Y., and Kim, W.T. (2011). The *Arabidopsis* sn-1-specific mitochondrial acylhydrolase AtDLAH is positively correlated with seed viability. J. Exp. Bot. **62:** 5683–5698.

Sharova, E.I. (2007). Expansins: proteins involved in cell wall softening during plant growth and morphogenesis. Russ. J. Plant Physiol. **54:** 713–727.

Shi, H., Liu, R., Xue, C., Shen, X., Wei, N., Deng, X.W., and Zhong, S. (2016a). Seedlings transduce the depth and mechanical pressure of covering soil using COP1 and ethylene to regulate EBF1/EBF2 for soil emergence. Curr. Biol. **26:** 139–149.

Shi, H., Shen, X., Liu, R., Xue, C., Wei, N., Deng, X.W., and Zhong, S. (2016b). The red light receptor Phytochrome B directly enhances Substrate-E3 Ligase interactions to attenuate ethylene responses. Dev. Cell **39:** 597–610.

Singh, A., Baranwal, V., Shankar, A., Kanwar, P., Ranjan, R., Yadav, S., Pandey, A., Kapoor, S., and Pandey, G.K. (2012). Rice phospholipase A superfamily: organization, phylogenetic and expression analysis during abiotic stresses and development. PLoS One **7:** e30947.

Song, S., Qi, T., Wasternack, C., and Xie, D. (2014a). Jasmonate signaling and crosstalk with gibberellin and ethylene. Curr. Opin. Plant Biol. **21:** 112–119.

Song, S., Huang, H., Gao, H., Wang, J., Wu, D., Liu, X., Yang, S., Zhai, Q., Li, C., Qi, T., and Xie, D. (2014b). Interaction between MYC2 and ETHYLENE INSENSITIVE3 modulates antagonism between jasmonate and ethylene signaling in *Arabidopsis.* Plant Cell **26:** 263–279.

Staswick, P.E., Tiryaki, I., and Rowe, M.L. (2002). Jasmonate response locus *JAR1* and several related *Arabidopsis* genes encode enzymes of the firefly luciferase superfamily that show activity on jasmonic, salicylic, and indole-3-acetic acids in an assay for adenylation. Plant Cell **14:** 1405–1415.

Sun, J., Ma, Q., and Mao, T. (2015). Ethylene regulates the *Arabidopsis* microtubule-associated protein WAVE-DAMPENED2-LIKE5 in etiolated hypocotyl elongation. Plant Physiol. **169:** 325–337.

Svyatyna, K., and Riemann, M. (2012). Light-dependent regulation of the jasmonate pathway. Protoplasma **249** (Suppl 2): S137–S145.

Takahashi, N. (1978). Adaptive importance of mesocotyl and coleoptile growth in rice under different moisture regimes. Aust. J. Plant Physiol. **5:** 511–517.

Takano, M., Kanegae, H., Shinomura, T., Miyao, A., Hirochika, H., and Furuya, M. (2001). Isolation and characterization of rice phytochrome A mutants. Plant Cell **13:** 521–534.

Vreeburg, R.A., Benschop, J.J., Peeters, A.J., Colmer, T.D., Ammerlaan, A.H., Staal, M., Elzenga, T.M., Staals, R.H., Darley, C.P., McQueen-Mason, S.J., and Voesenek, L.A. (2005). Ethylene regulates fast apoplastic acidification and expansin A transcription during submergence-induced petiole elongation in *Rumex palustris.* Plant J. **43:** 597–610.

Wang, C., Zien, C.A., Afitlhile, M., Welti, R., Hildebrand, D.F., and Wang, X. (2000). Involvement of phospholipase D in wound-induced accumulation of jasmonic acid in *Arabidopsis.* Plant Cell **12:** 2237–2246.

Watanabe, H., Takahashi, K., and Saigusa, M. (2001). Morphological and anatomical effects of abscisic acid (ABA) and fluridone (FLU) on the growth of rice mesocotyls. Plant Growth Regul. **34:** 273–275.

Wei, F.J., et al. (2016). Somaclonal variation does not preclude the use of rice transformants for genetic screening. Plant J. **85:** 648–659.

Wen, X., Zhang, C., Ji, Y., Zhao, Q., He, W., An, F., Jiang, L., and Guo, H. (2012). Activation of ethylene signaling is mediated by nuclear translocation of the cleaved EIN2 carboxyl terminus. Cell Res. **22:** 1613–1616.

Wilen, R.W., Ewan, B.E., and Gusta, L.V. (1994). Interaction of abscisic acid and jasmonic acid on the inhibition of seed germination and the induction of freezing tolerance. Can. J. Bot. **72:** 1009–1017.

Wu, J., et al. (2015). Genome-wide Association Study (GWAS) of mesocotyl elongation based on re-sequencing approach in rice. BMC Plant Biol. **15:** 218.

Wuriyanghan, H., et al. (2009). The ethylene receptor ETR2 delays floral transition and affects starch accumulation in rice. Plant Cell **21:** 1473–1494.

Yang, C., Lu, X., Ma, B., Chen, S.Y., and Zhang, J.S. (2015a). Ethylene signaling in rice and *Arabidopsis*: conserved and diverged aspects. Mol. Plant **8:** 495–505.

Yang, C., Ma, B., He, S.J., Xiong, Q., Duan, K.X., Yin, C.C., Chen, H., Lu, X., Chen, S.Y., and Zhang, J.S. (2015b). *MAOHUZI6/ETHYLENE INSENSITIVE3-LIKE1* and *ETHYLENE INSENSITIVE3-LIKE2* regulate ethylene response of roots and coleoptiles and negatively affect salt tolerance in rice. Plant Physiol. **169:** 148–165.

Yin, C.C., Ma, B., Wang, W., Xiong, Q., Zhao, H., Chen, S.Y., and Zhang, J.S. (2016). RNA extraction and preparation in rice (*Oryza sativa*). Curr. Protoc. Plant Biol. **1:** 411–418.

Yin, C.C., et al. (2015). Ethylene responses in rice roots and coleoptiles are differentially regulated by a carotenoid isomerase-mediated abscisic acid pathway. Plant Cell **27:** 1061–1081.

Yuan, Z., and Zhang, D. (2015). Roles of jasmonate signalling in plant inflorescence and flower development. Curr. Opin. Plant Biol. **27:** 44–51.

Zhang, B., Wu, S., Zhang, Y., Xu, T., Guo, F., Tang, H., Li, X., Wang, P., Qian, W., and Xue, Y. (2016). A high temperature-dependent mitochondrial lipase EXTRA GLUME1 promotes floral phenotypic robustness against temperature fluctuation in rice (*Oryza sativa* L.). PLoS Genet. **12:** e1006152.

Zhang, X., Zhu, Z., An, F., Hao, D., Li, P., Song, J., Yi, C., and Guo, H. (2014). Jasmonate-activated MYC2 represses ETHYLENE

INSENSITIVE3 activity to antagonize ethylene-promoted apical hook formation in *Arabidopsis.* Plant Cell **26:** 1105–1117.

Zhong, S., Zhao, M., Shi, T., Shi, H., An, F., Zhao, Q., and Guo, H. (2009). EIN3/EIL1 cooperate with PIF1 to prevent photo-oxidation and to promote greening of *Arabidopsis* seedlings. Proc. Natl. Acad. Sci. USA **106:** 21431–21436.

Zhong, S., Shi, H., Xue, C., Wei, N., Guo, H., and Deng, X.W. (2014). Ethylene-orchestrated circuitry coordinates a seedling's response to soil cover and etiolated growth. Proc. Natl. Acad. Sci. USA **111:** 3913–3920.

Zhu, C., Gan, L., Shen, Z., and Xia, K. (2006). Interactions between jasmonates and ethylene in the regulation of root hair development in *Arabidopsis.* J. Exp. Bot. **57:** 1299–1308.

Zhu, Z., et al. (2011). Derepression of ethylene-stabilized transcription factors (EIN3/EIL1) mediates jasmonate and ethylene signaling synergy in *Arabidopsis.* Proc. Natl. Acad. Sci. USA **108:** 12539–12544.

Ziegler, J., Stenzel, I., Hause, B., Maucher, H., Hamberg, M., Grimm, R., Ganal, M., and Wasternack, C. (2000). Molecular cloning of allene oxide cyclase. The enzyme establishing the stereochemistry of octadecanoids and jasmonates. J. Biol. Chem. **275:** 19132–19138.